SUPPLEMENTARY DATA

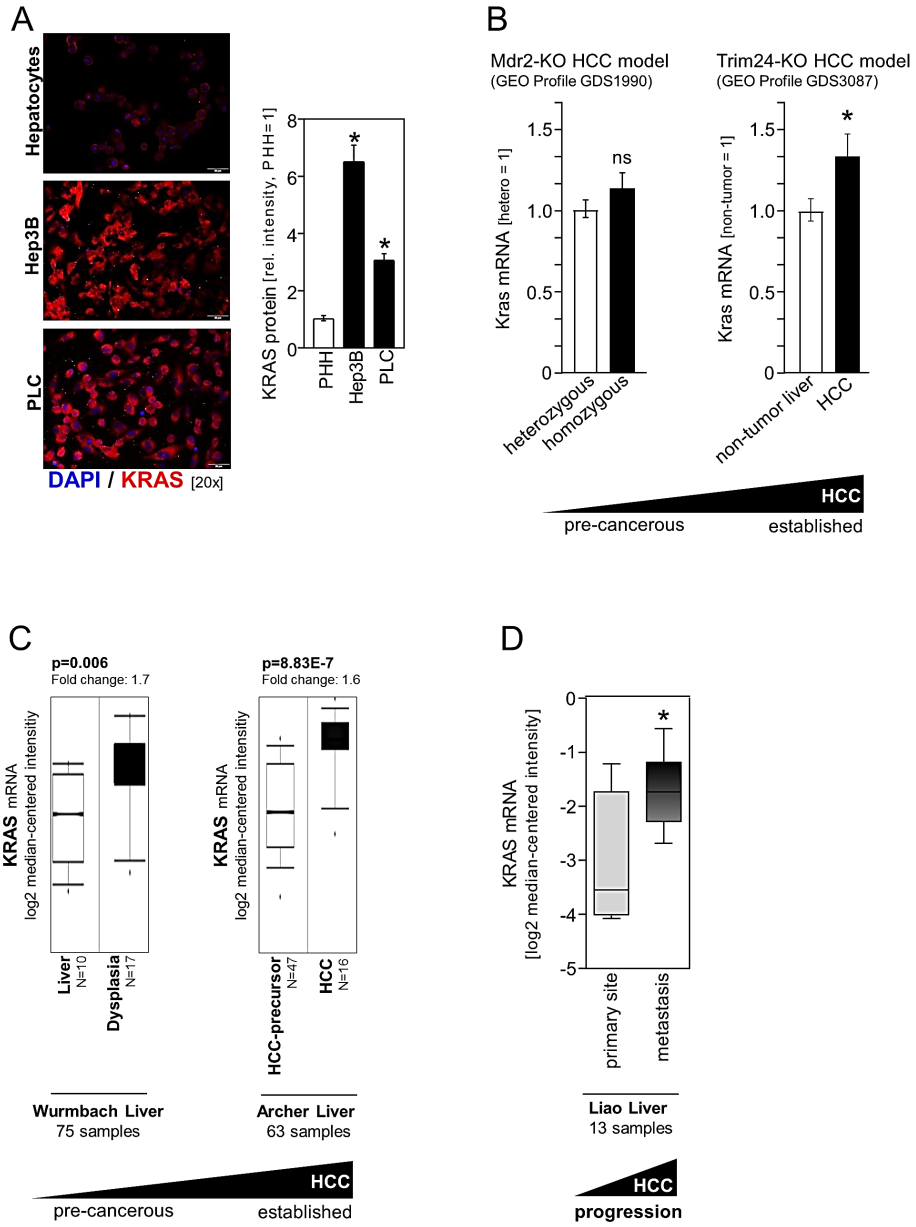

Figure S1 KRAS expression in HCC.

(**A**) Representative images depicting KRAS protein expression in HCC cell lines (Hep3B, PLC) as compared to primary human hepatocytes (PHH) and densitometric quantification of relative fluorescence intensity. (*p<0.05 compared with PHH). (**B**) To address KRAS expression levels during HCC development, a pre-cancerous murine dataset comparing heterozygous and homozygous Mdr2 knockout (KO) mice was used (left side). Moreover, KRAS expression was analyzed in a dataset (Trim24-deficient murine HCC model) comparing HCC samples and non-tumorous control liver tissues (right side). (Ns: non-significant. *p<0.05) (**C**) Oncomine^{TM} human cancer microarray database analysis of two patient datasets depicting KRAS mRNA expression levels in pre-cancerous liver dysplasia compared to non-dysplastic liver tissues (left side) and in HCC tissues compared to HCC-precursors (right side). (**D**) Oncomine^{TM} human cancer microarray database derived dataset comparing KRAS expression in metastasis and primary HCC. (*p<0.05 compared with "primary site").

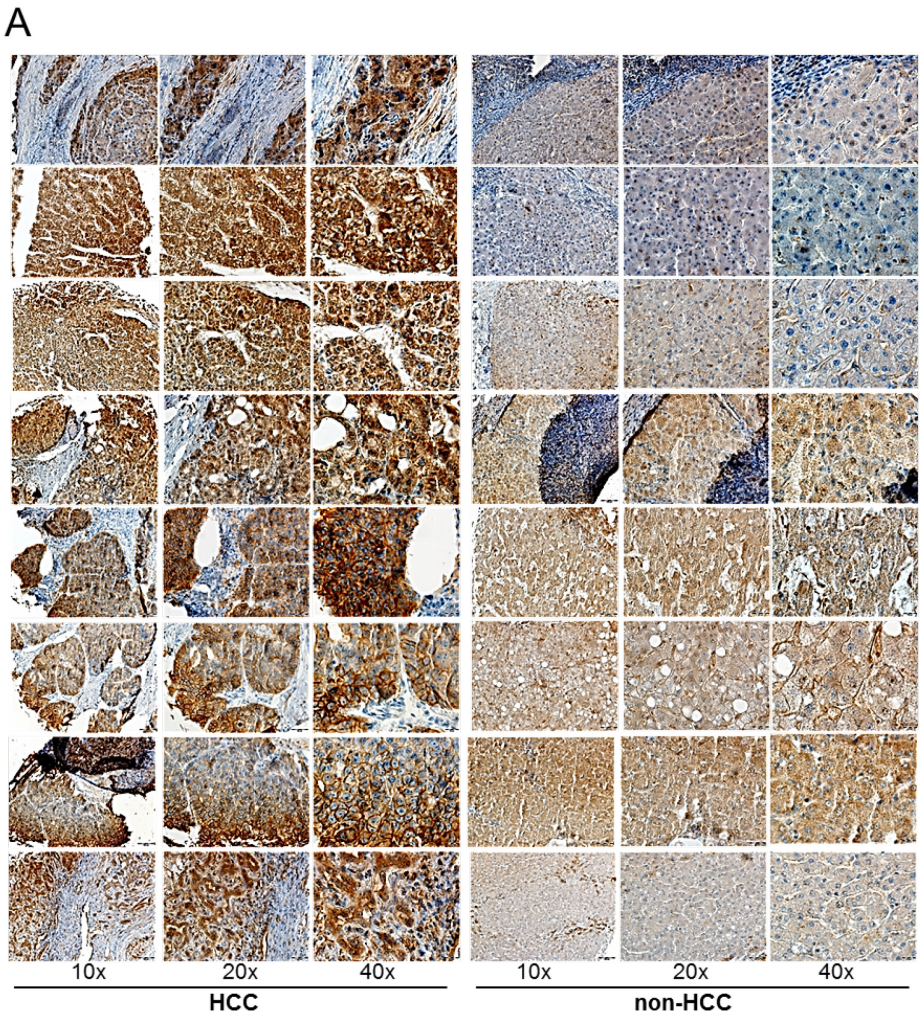

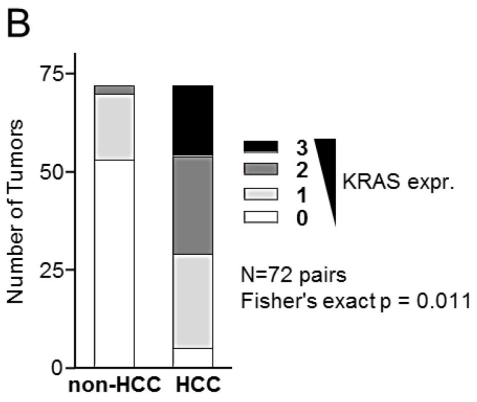

	0	1	2	3
non-HCC	53.0	17.0	2.0	0.0
HCC	5.0	24.0	25.0	18.0

Numbers of Tumors

C

Tumor Stage

	1	2	3	4
low KRAS	56.7	30.0	13.3	0.0
high KRAS	11.3	30.2	54.7	3.9

% Tumors

D

KRAS expr. score

Size	0	1	2	3
< 5 cm	7.1	52.4	26.2	14.3
> 5 cm	0.0	6.7	50.0	43.3

% Tumors

Figure S2 Tissue micro array (TMA) analysis of KRAS protein expression in HCC. **(A)** Exemplary images of paired (per line) HCC and corresponding non-tumorous liver tissues. **(B-D)** Quantification and statistical information for KRAS expression score (0-4) in HCC as compared to corresponding non-tumorous liver tissues ("non-HCC") (B), tumor stages (1-4) in low and high KRAS expression groups (C) and KRAS expression score (0-4) in small (<5 cm) and large (>5 cm) tumor size groups (D). A detailed description of scoring and quantification is depicted in the "Methods" section.

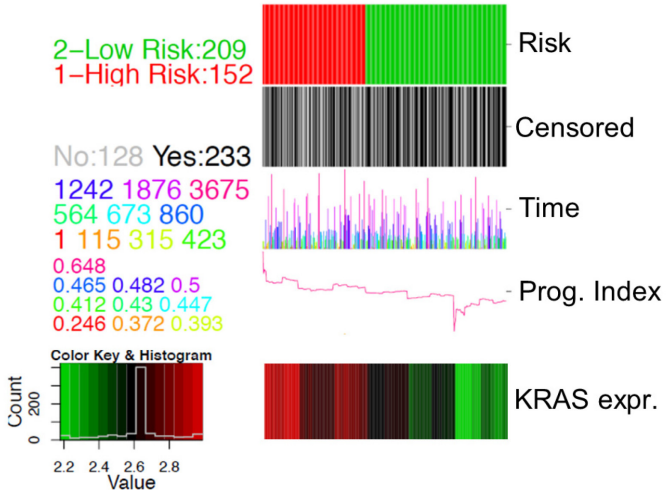

Figure S3 ***In silico*** **analysis of KRAS expression in HCC.**
SurvExpress-Biomarker validation for cancer gene expression" database analysis of a HCC TCGA ("The Cancer Genome Atlas") dataset. The Heatmap shows KRAS expression according to prognostic index and stratification into "low risk" and "high risk" group.

A

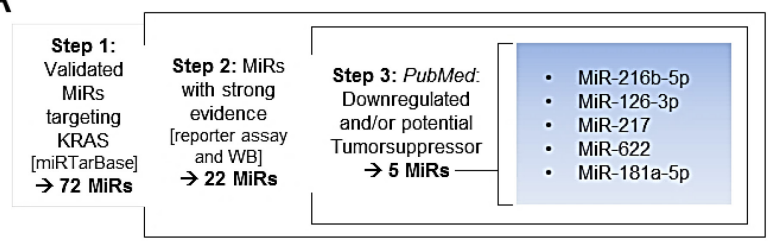

B

	MiR-216b-5p	MiR-126-3p	MiR-217	MiR-622	MiR-181a-5p
number of datasets	6	1	6	6	1
probe IDs	17849, 45381, 20785, ILMN_3168550, ILM31868550, 4466	hsa-miR-126-3p	59749, 50397, 45097, hsa-miR-217-precNo2, 19016, 57186	17493, 10311, 646, hsa-miR-622, ILMN_3167141	hsa-miR-181A-5P
Geo IDs	GSE37405, GSE59334, GSE39058, GSE39040	GSE43732	GSE59334, GSE13937, GSE37405	GSE37405, GSE59334, GSE36682, GSE21849, GSE39058, GSE39040	GSE43732
cancer types	Breast Cancer (1), Melanoma (3), Osteosarcoma (2)	Esophangeal Carcinoma (1)	Melanoma (4), Esophageal Carcinoma (1), Breast Cancer (1)	Breast Cancer (1), Melanoma (1), Nasopharyngeal Carcinoma (1), Diffuse B Cell Lymphoma (1), Osteosarcoma (2)	Esophangeal Carcinoma (1)
effects on overall survival, didease free survival, and/or tumor recurrence	**3 positive, 3 negative**	**negative**	**3 positive, 3 negative**	**6 positive [100%]**	**negative**

C

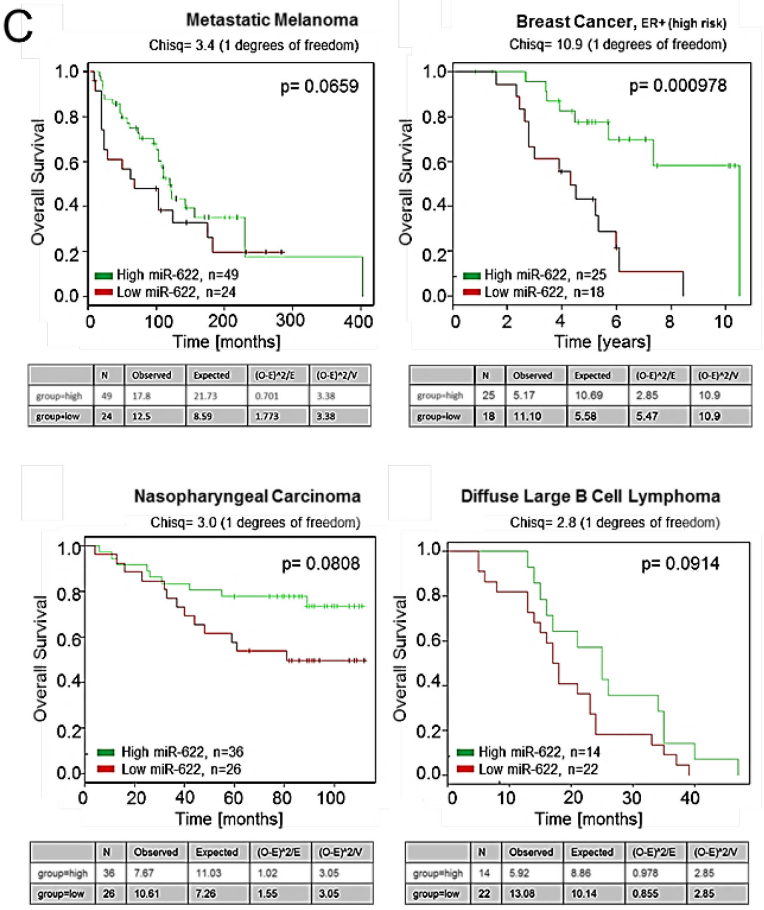

	N	Observed	Expected	(O-E)^2/E	(O-E)^2/V
group=high	49	17.8	21.73	0.701	3.38
group=low	24	12.5	8.59	1.773	3.38

	N	Observed	Expected	(O-E)^2/E	(O-E)^2/V
group=high	25	5.17	10.69	2.85	10.9
group=low	18	11.10	5.58	5.47	10.9

	N	Observed	Expected	(O-E)^2/E	(O-E)^2/V
group=high	36	7.67	11.03	1.02	3.05
group=low	26	10.61	7.26	1.55	3.05

	N	Observed	Expected	(O-E)^2/E	(O-E)^2/V
group=high	14	5.92	8.86	0.978	2.85
group=low	22	13.08	10.14	0.855	2.85

Figure S4 MiR-622 targets KRAS in HCC. (A) Multistep *in silico* analysis of validated microRNAs targeting KRAS (using miRTarBase database as described in the "Methods" section). **(B,C)** Using the MIRUMIR database, selected microRNAs as depicted in (A) (miR-216b-5p, miR-126-3p, miR-217, miR-622, and miR-181a-5p) were analyzed. The table (B) shows the number of available TCGA datasets, the probe IDs, the Geo IDs, the according cancer types, and the summarized effects on overall survival, disease free survival, and/or tumor recurrence. Kaplan-Meier curves (C) depict overall survival of cancer patients with high miR-622 as compared to low miR-622 expression in 4 different cancer types (metastatic melanoma, breast cancer, nasopharyngeal carcinoma, and diffuse large B cell lymphoma). Chisq= chi square.

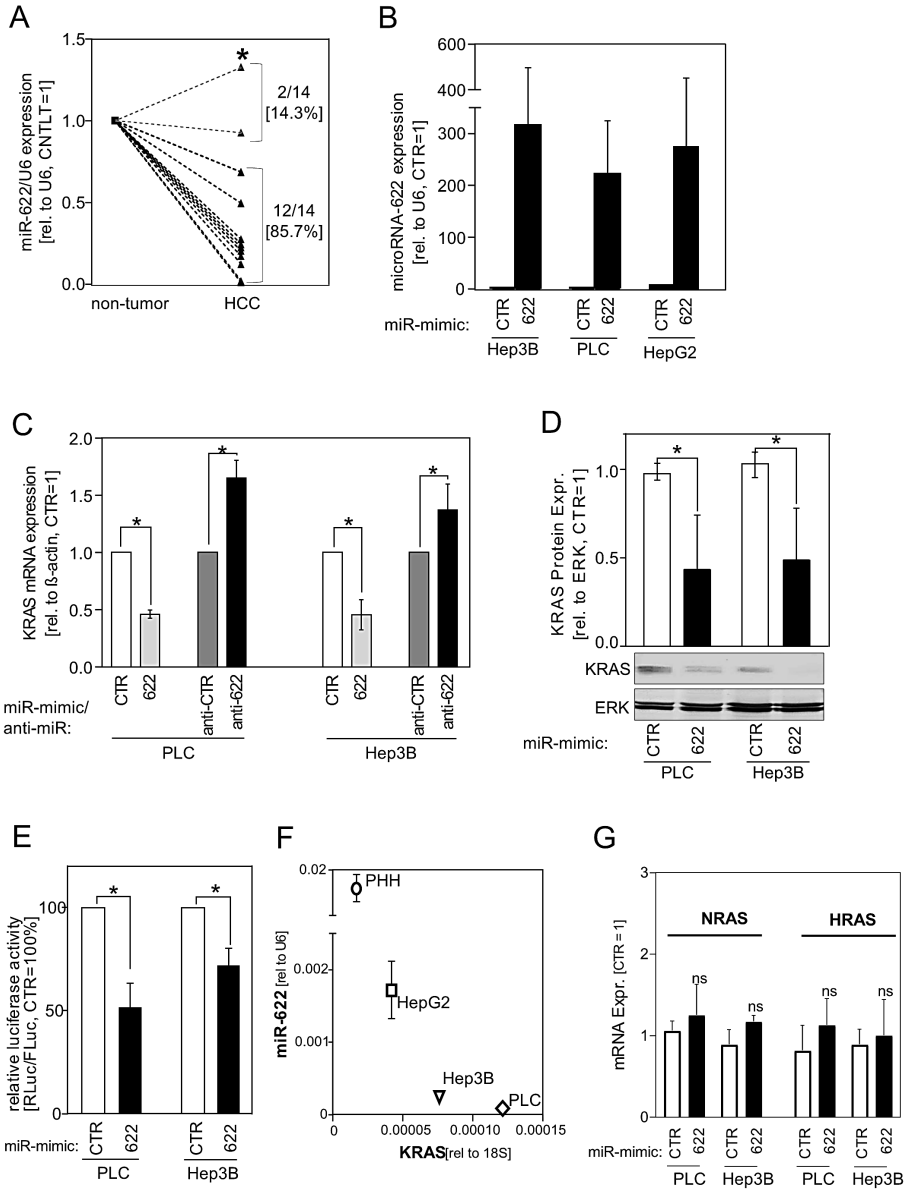

Figure S5 MiR-622 expression and regulation of KRAS expression in HCC. (A) Quantitative RT-PCR analysis depicting miR-622 expression levels in pairs of patient derived HCC samples and corresponding non-tumorous liver tissue samples (n=14 pairs). **(B)** Quantitative RT-PCR analysis of miR-622 levels of HCC cell lines (Hep3B, PLC and HepG2) after miR-622 (622) or control-miR (CTR) transfection, respectively. **(C,D)** For re-expression or inhibition of miR-622 in HCC cell lines (PLC, Hep3B), cells were transfected with control-miR (CTR), miR-622 (622), anti-control-miR (anti-CTR), or anti-miR-622 (anti-622), respectively. Quantitative RT-PCR analysis (C) and Western blot analysis (D) show KRAS mRNA and protein expression levels. **(E)** Luciferase reporter assay was performed using a vector encoding for renilla luciferase (RLuc) and the 3'UTR of the KRAS gene including the predicted miR-622 binding sites. A firefly luciferase control plasmid vector was used (FLuc) for normalization. MiR-622 (622) or control-miR (CTR) was co-transfected. The relative luciferase activity (RLuc/FLuc) was set as 100% in control-miR (CTR) transfected cells. (**F**) KRAS (x-axis) and miR-622 (y-axis) expression in primary human hepatocytes and HCC cell lines (Hep3B, HepG2, PLC). (**G**) NRAS and HRAS mRNA expression (qRT-PCR) in HCC cells (PLC, Hep3B) after transfection of a miR-622-mimic as compared to control-transfected cells (CTR). (Ns: non-significant. *p<0.05 compared with control).

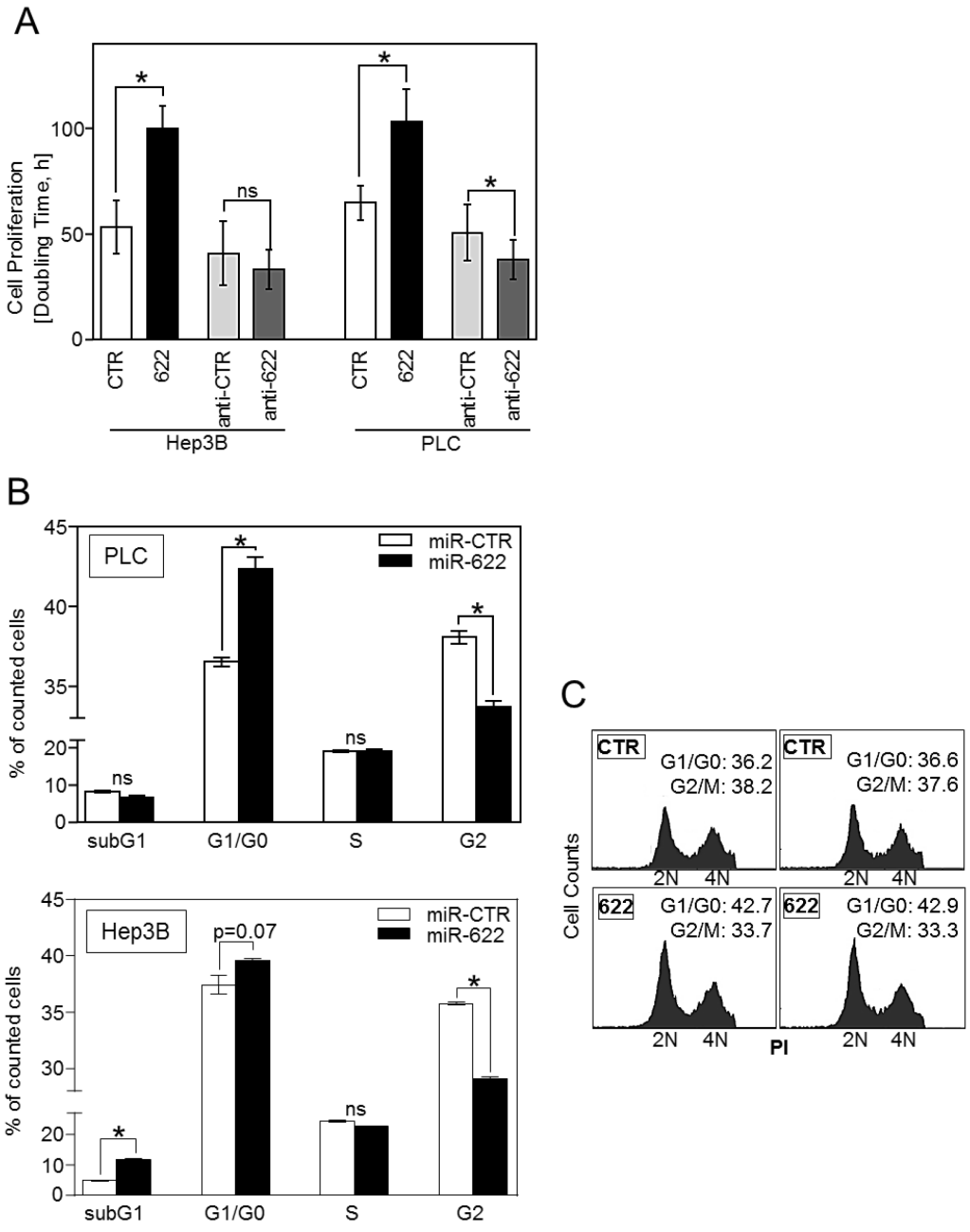

Figure S6 MiR-622 function on proliferation in HCC.

For re-expression or inhibition of miR-622 in HCC cell lines (PLC, Hep3B), cells were transfected with control-miR (CTR), miR-622 (622), anti-control-miR (anti-CTR), or anti-miR-622 (anti-622), respectively. **(A)** Real-time cell proliferation. The "Doubling time" summarizes the proliferative ability of tumor cells. **(B,C)** Flow cytometric propidium iodide staining depicts percentage of cells (PLC, Hep3B) in cell cycle fractions (Sub G1, G0/G1, S, and G2) after miR-622 (622) transfection as compared to controls (CTR) (B) and exemplary images (C). (Ns: non-significant. *p<0.05 compared with control).

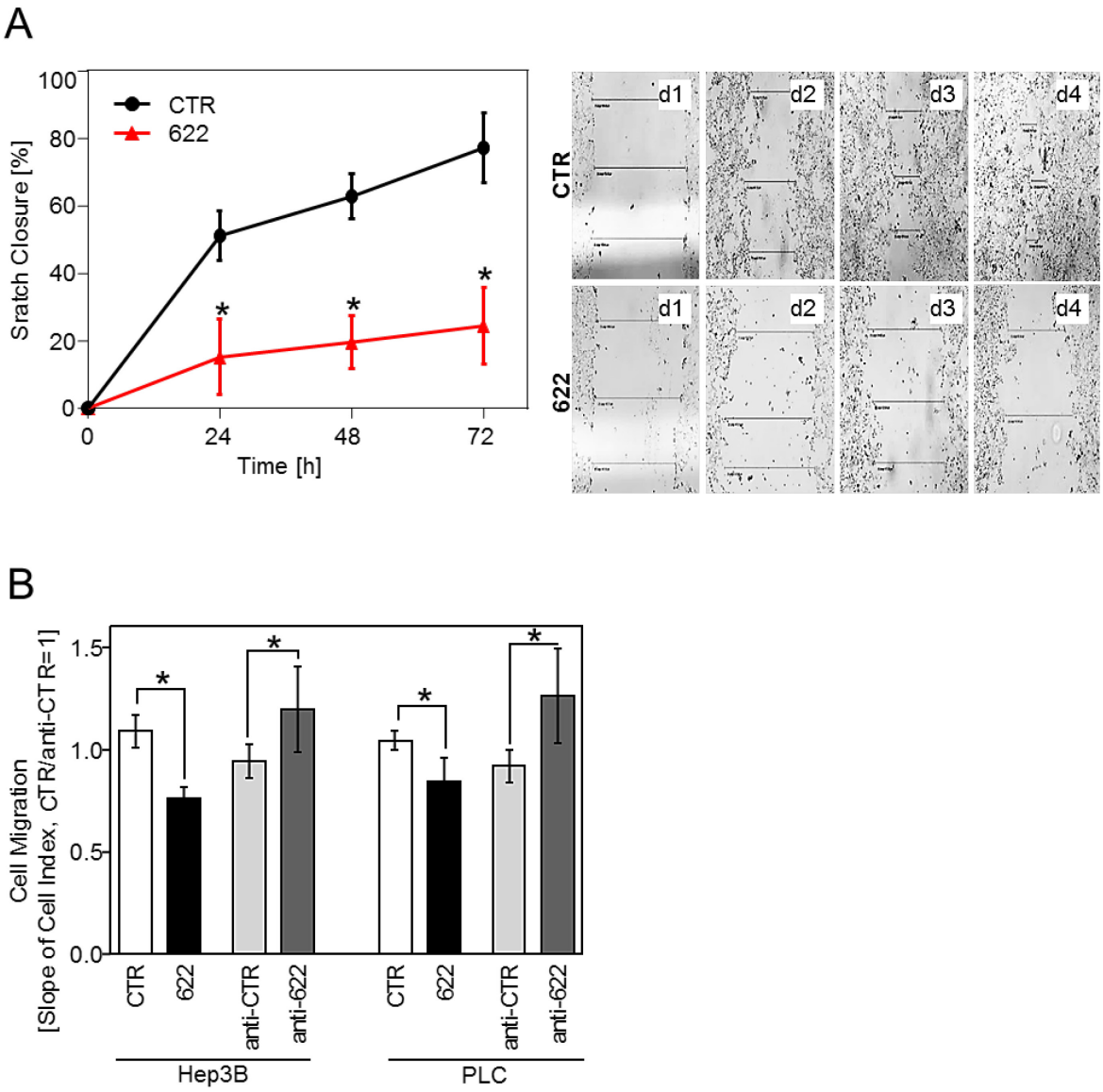

Figure S7 MiR-622 effects on cell migration in HCC.
(A) Scratch closure assay of control transfected (CTR) Hep3B cells as compared to cells with re-expressed miR-622 (622), and exemplary images. **(B)** Cell migration of control-transfected (CTR) or miR-622-/anti-miR-622-transfected (622/anti-622) Hep3B and PLC cells, respectively; analyzed with the xCELLigence system. (*p<0.05 compared with control).

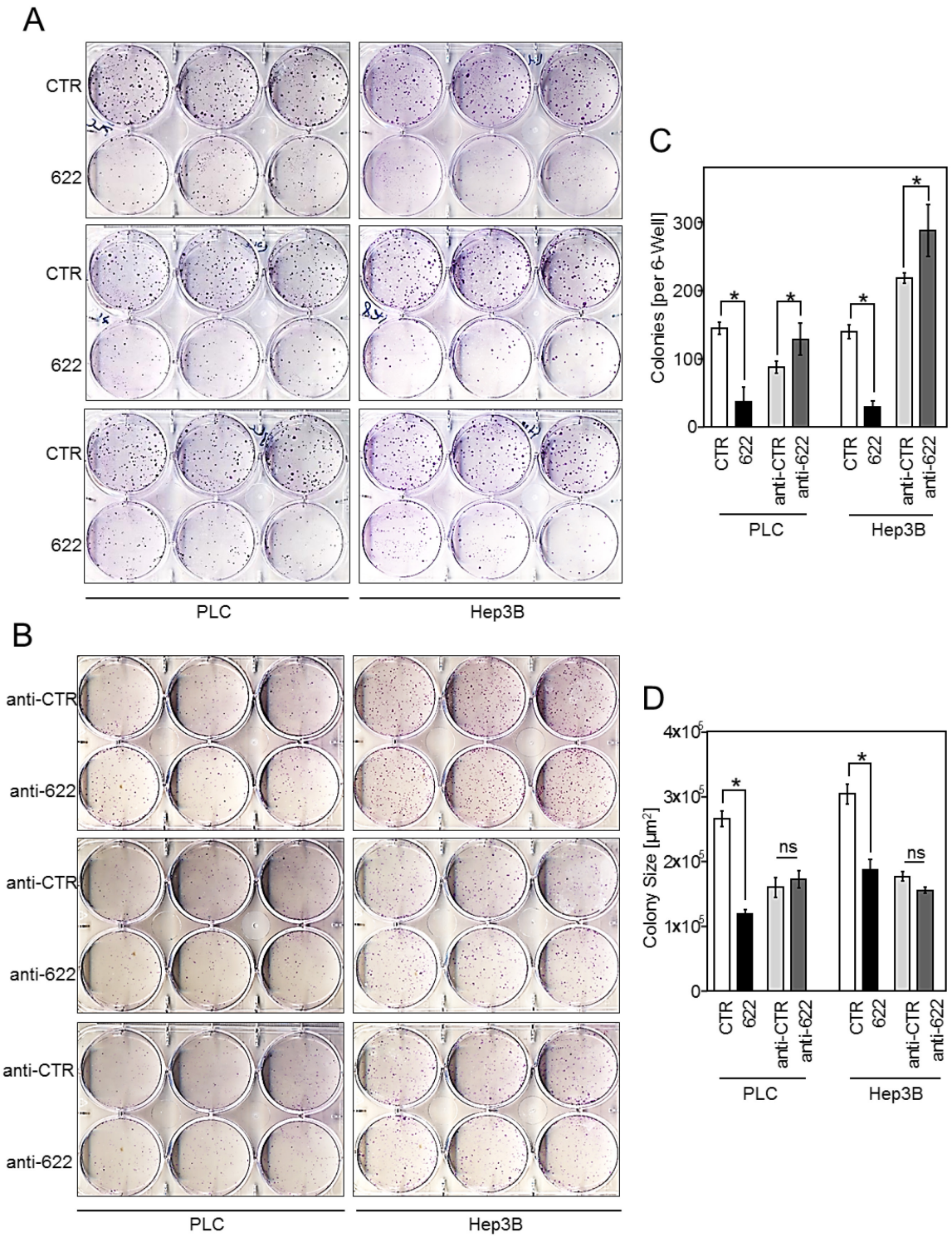

Figure S8 MiR-622 effects on anchorage-dependent clonogenicity in HCC.
(A,B) Functional analysis of miR-622 effects on hepatocellular carcinoma cell lines (Hep3B and PLC) was performed after re-expression of miR-622 (622) (A) or inhibition of endogenous miR-622 activity by using transfection of an anti-miR-622 (anti-622) (B) and according controls (control-miR=CTR or control-anti-miR=anti-CTR), respectively. (A) and (B) depict 3 independent anchorage-dependent clonogenic assays for PLC and Hep3B for each treatment (with 3 replicate 6-wells per experiment). **(C,D)** Quantification of colony number (C) and colony sizes (D) according to (A) and (B). (Ns: non-significant. *$p<0.05$ compared with control).

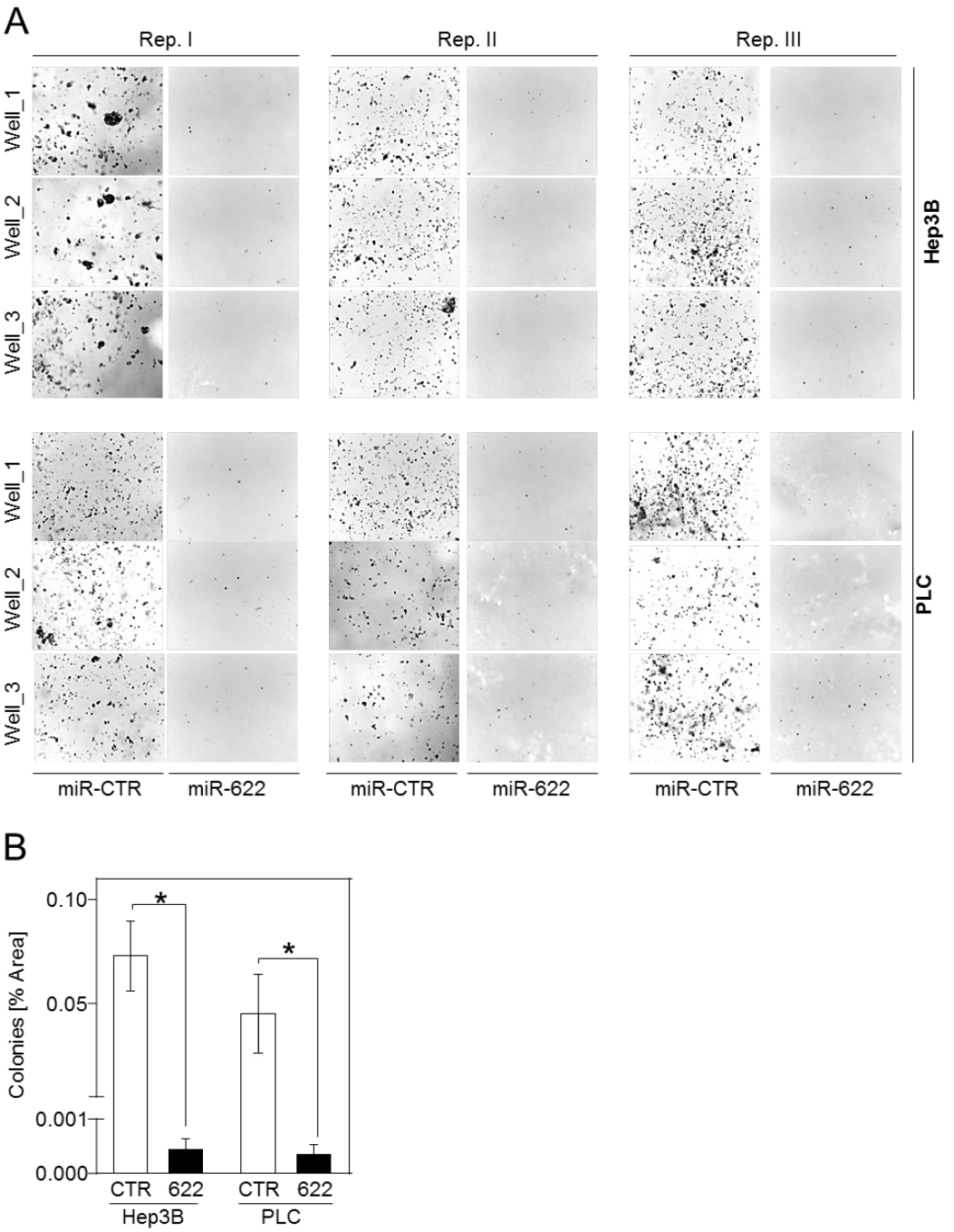

Figure S9 MiR-622 effects on anchorage-independent clonogenicity in HCC. Functional analysis of miR-622 effects on hepatocellular carcinoma cell lines (Hep3B, HepG2 and PLC) was performed after re-expression of miR-622 (622) and according controls (control-miR=CTR). **(A)** Exemplary images of 3 independent anchorage-independent colony forming assays for PLC and Hep3B cells, respectively. **(B)** Quantification of colonies. (*$p<0.05$ compared with control).

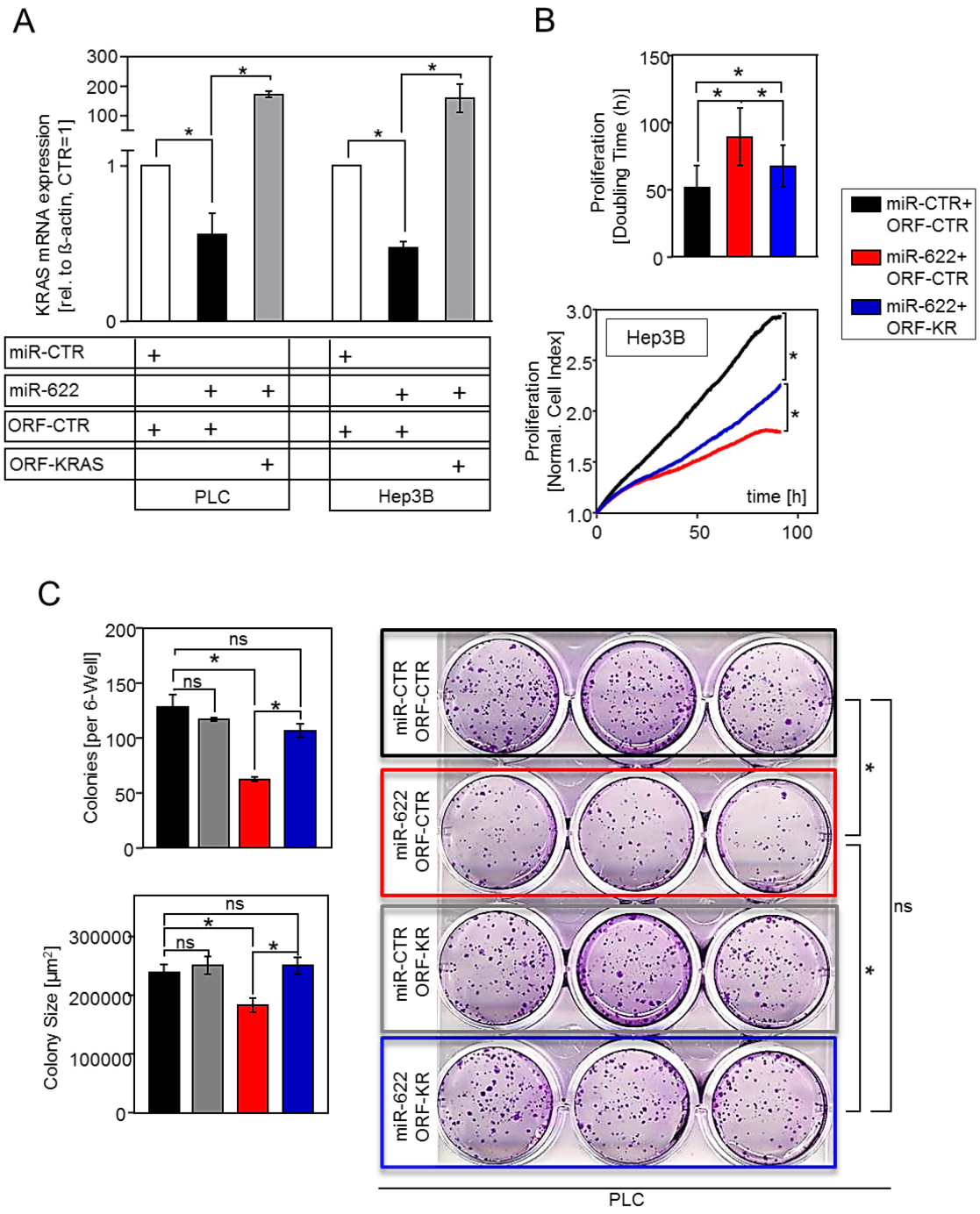

Figure S10 MiR-622 effects and KRAS "rescue" assays.
PLC and Hep3B were transfected in 4 different groups: i) control miR + control vector (miR-CTR + ORF-CTR), ii) control miR + KRAS-Open Reading Frame (miR-CTR + ORF-KR) containing vector for KRAS overexpression, iii) miR-622 + control vector, and iv) miR-622 + KRAS-ORF vector. **(A)** Quantitative RT-PCR analysis of KRAS mRNA expression levels confirms that miR-622 + ORF-CTR reduces KRAS expression, while ORF-KRAS transfection is sufficient to overexpress KRAS expression in the presence of miR-622 re-expression. **(B)** Real-time cell proliferation. Exemplary proliferation curves and "Doubling times" (summarizing the proliferative ability) are depicted for Hep3B. **(C)** Colony number, colony size, and exemplary images are shown for anchorage-dependent clonogenic assays for PLC. (Ns: non-significant. *p<0.05 compared with control).

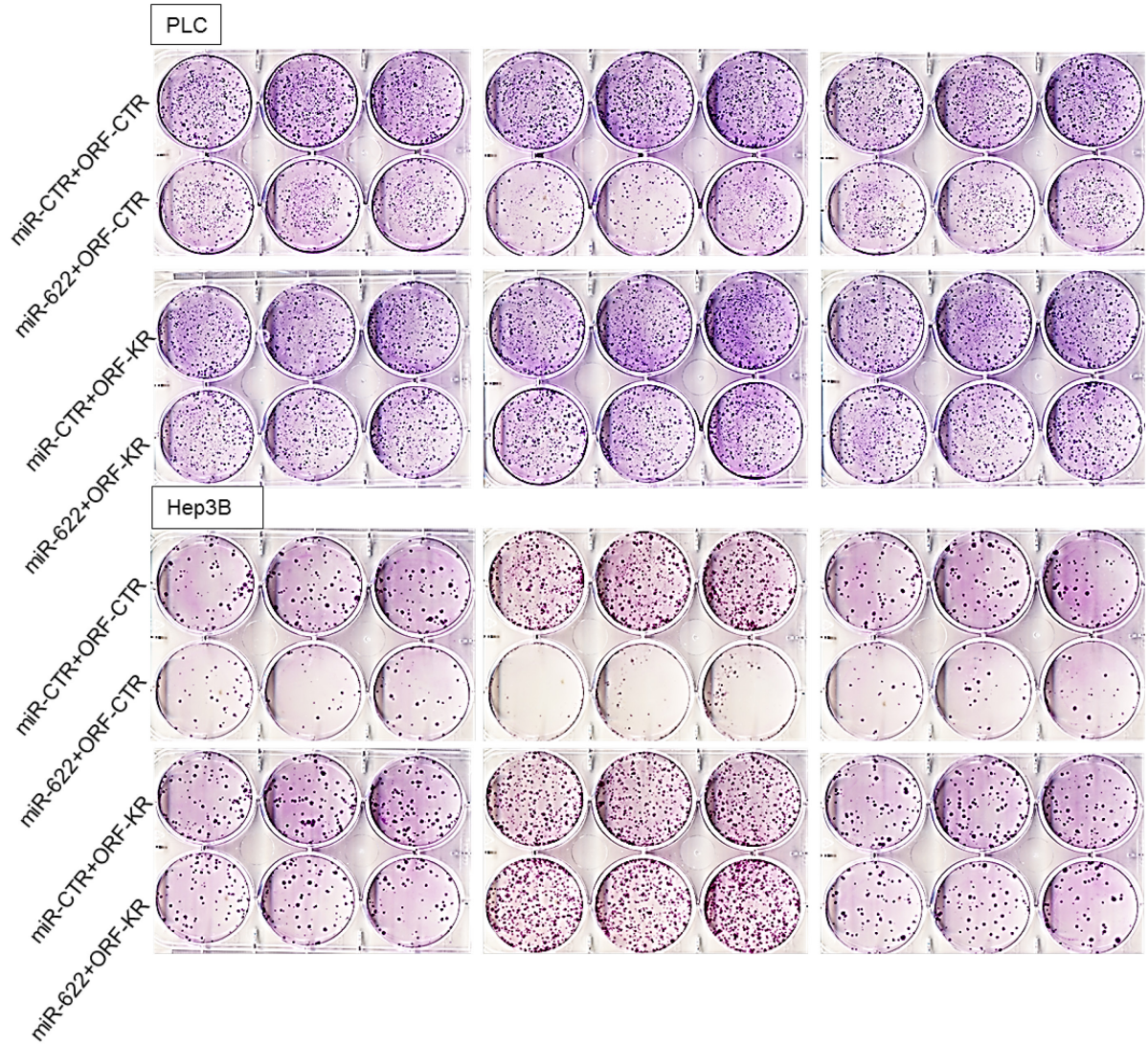

Figure S11 KRAS "rescue" of miR-622 effects on clonogenicity in HCC.
HCC cell lines PLC and Hep3B were transfected in 4 different groups: i) control miR + control vector (miR-CTR + ORF-CTR), ii) control miR + KRAS-Open Reading Frame (miR-CTR + ORF-KR) containing vector for KRAS overexpression, iii) miR-622 + control vector, and iv) miR-622 + KRAS-ORF vector. Anchorage-dependent clonogenic assays for PLC (top) and Hep3B (Hep3B) (3 independent experiments with 3 replicate wells for each treatment are shown).

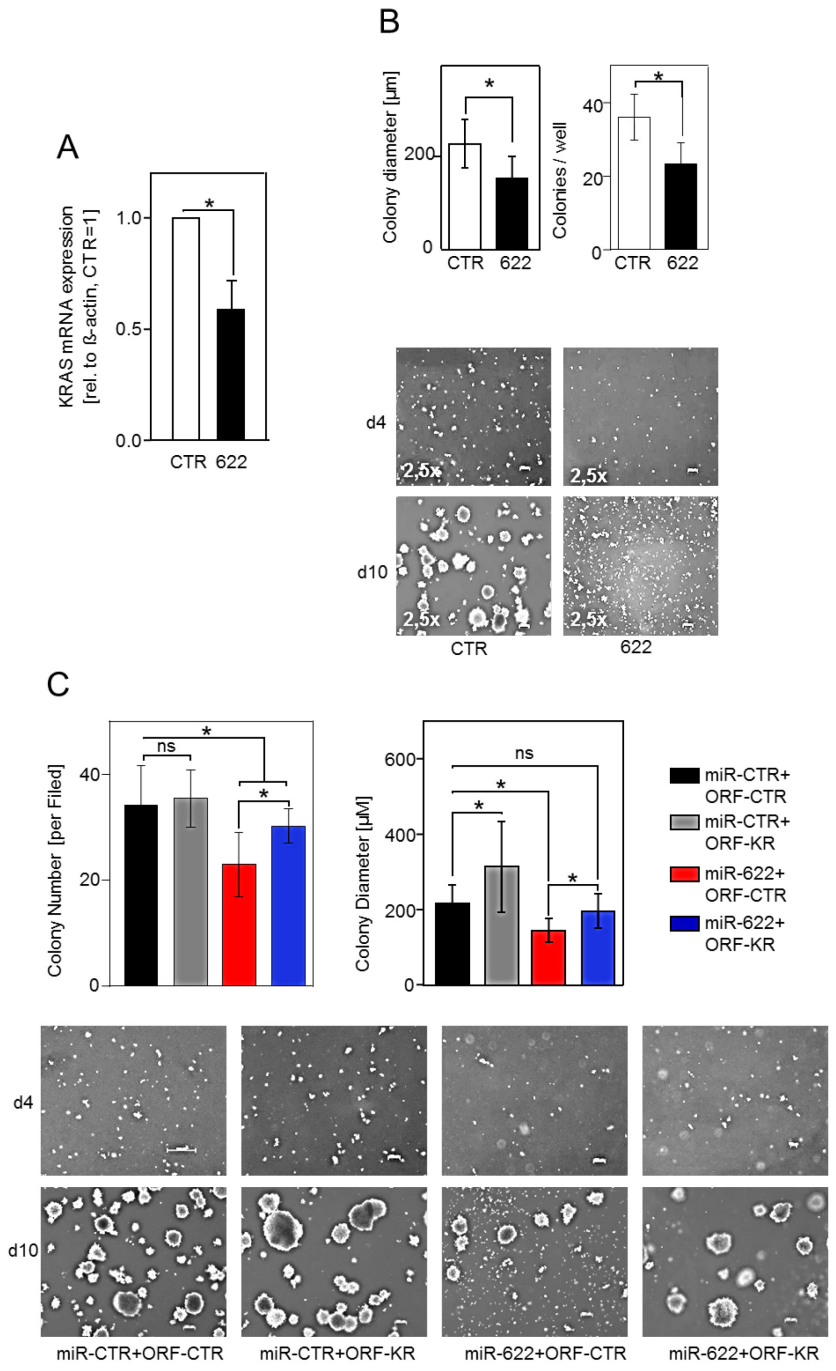

Figure S12 MiR-622 effects and KRAS "rescue" in additional HCC cells (HepG2). For further confirmation, additional experiments were performed in a third HCC cell line (HepG2). **(A)** MiR-622 (622)-induced KRAS-downregulation as compared to control-transfected (CTR) HepG2 cells (qRT-PCR). **(B)** Quantification of miR-622 (622) induced effects on colony size (diameter) and number (upper panels) and exemplary images (bottom panels) of anchorage-independent colony formation. **(C)** KRAS "Rescue" assays (anchorage-independent colony formation) in HepG2 cells. Colony number and sizes are quantified and exemplary images are shown. HepG2 cells were transfected in 4 different groups: i) control miR + control vector (miR-CTR + ORF-CTR), ii) control miR + KRAS-Open Reading Frame (miR-CTR + ORF-KR) containing vector for KRAS overexpression, iii) miR-622 + control vector, and iv) miR-622 + KRAS-ORF vector. (Ns: non-significant. *p<0.05 compared with control).

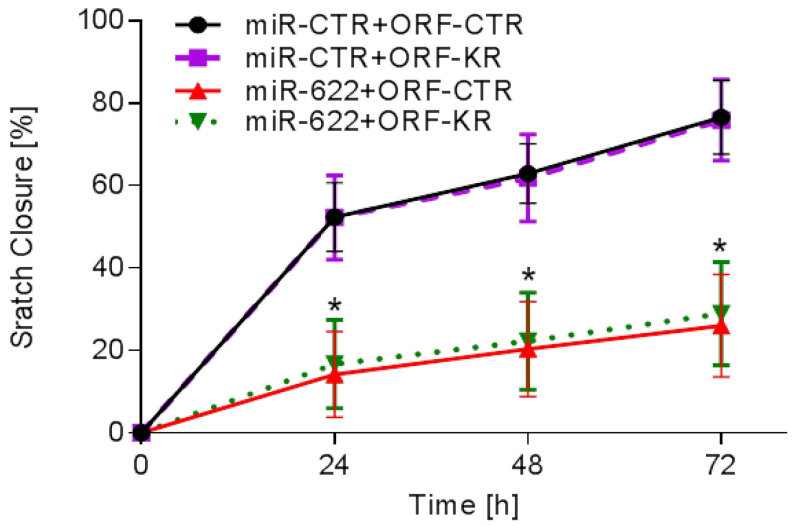

Figure S13 KRAS knockdown effects on cell migration and KRAS "rescue" effects on miR-622-mediated effects on migration.
Hep3B cells were transfected in 4 different groups: i) control miR + control vector (miR-CTR + ORF-CTR), ii) control miR + KRAS-Open Reading Frame (miR-CTR + ORF-KR) containing vector for KRAS overexpression, iii) miR-622 + control vector, and iv) miR-622 + KRAS-ORF vector. Subsequently, a scratch closure assay was performed. (*$p<0.05$ compared with control).

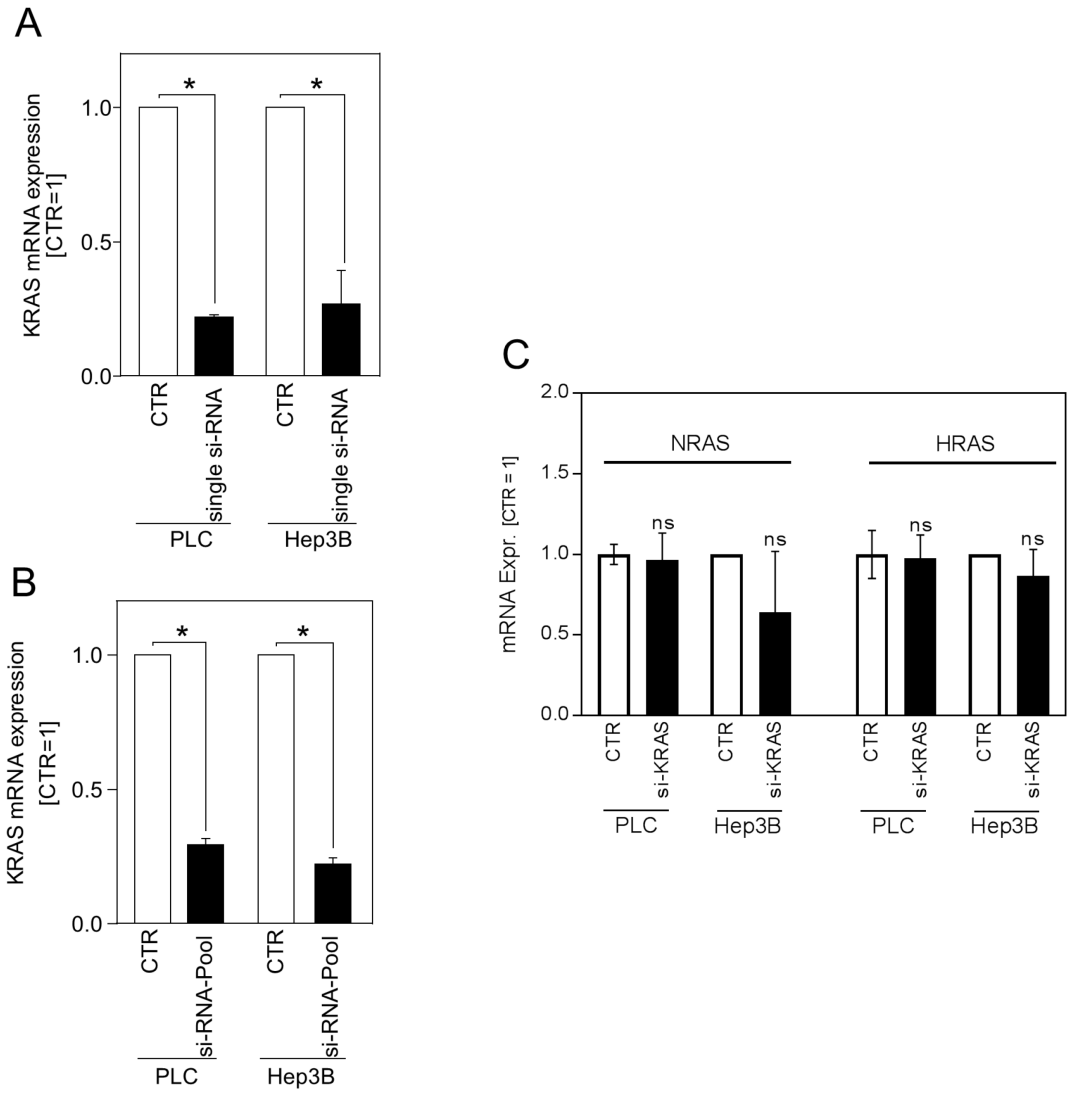

Figure S14 RNA-interference-mediated KRAS repression in HCC cell lines.
(A,B) Two different approaches of RNA-interference – a single si-RNA (A) and a si-RNA-Pool consisting of 30 si-RNAs against KRAS (B) – were used to avoid any bias or off-target effects. Quantitative RT-PCR analysis of KRAS mRNA levels of transfected HCC cell lines (PLC, Hep3B) is shown. CTR: control-transfected cells (single-control-si-RNA in (A) and si-RNA-control-Pool in (B)). (**C**) Expression of other RAS-isoforms besides KRAS were analyzed in HCC cells treated with si-RNA-pools directed against KRAS. This was performed to i) proof the isoform-specificity of the RNAi-mediated suppression as performed in this study and to ii) determine if there is a compensatory upregulation of other RAS-isoforms. Depicted are NRAS and HRAS mRNA expression levels (qRT-PCR) in HCC cells (PLC, Hep3B) after si-Pool-mediated KRAS knockdown (si-KRAS) as compared to control-transfected cells (CTR). (*$p<0.05$ compared with control).

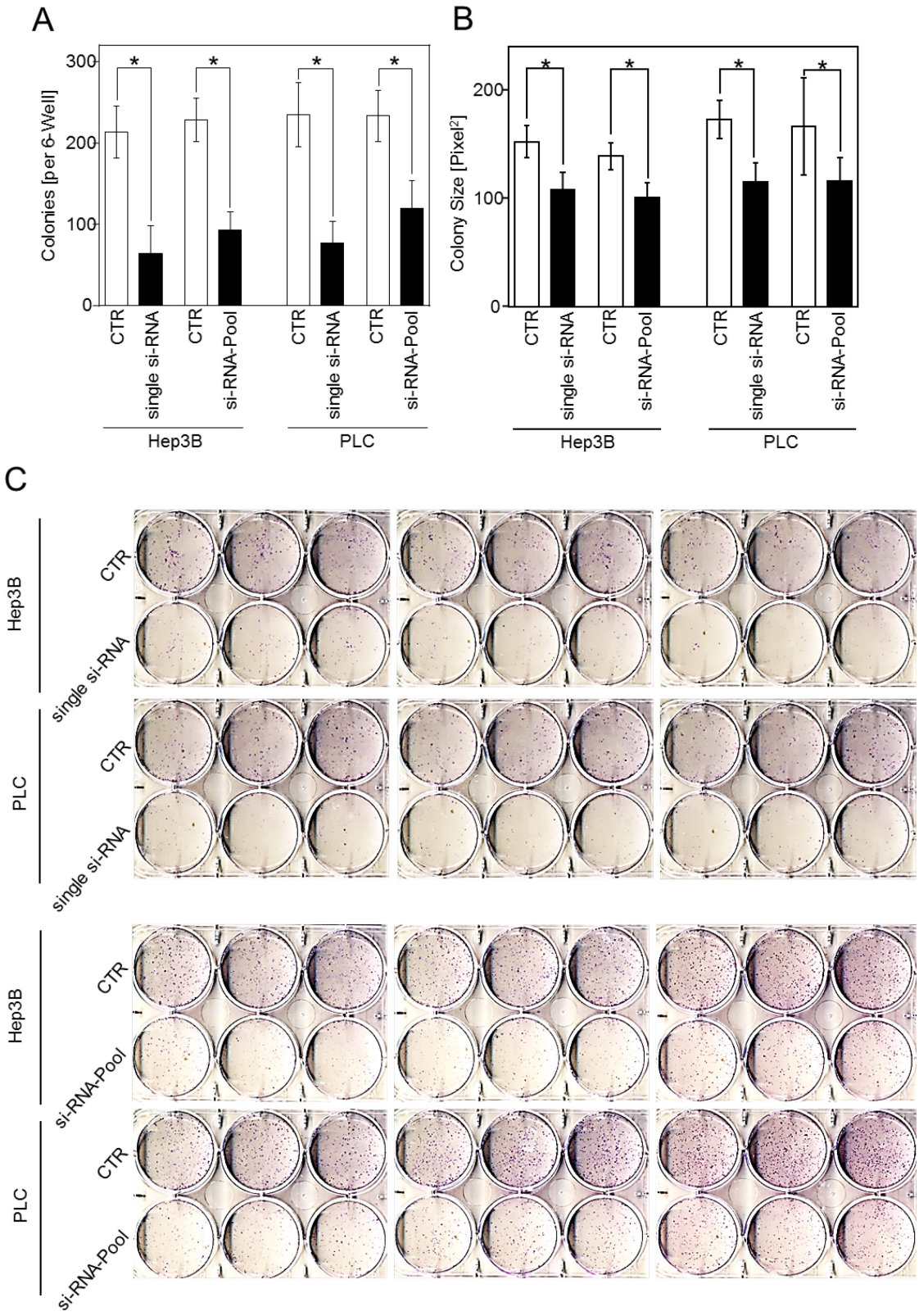

Figure S15 Effects of KRAS knockdown on anchorage-dependent clonogenicity in HCC cell lines.

Results are shown for PLC and Hep3B cells and both single-si-RNA and si-RNA-Pool-mediated KRAS suppression. **(A)** Quantification of colony number. **(B)** Quantification of colony size. **(C)** Exemplary images (9 replicate wells according to 3 independent experiments for each condition). (*$p<0.05$ compared with control).

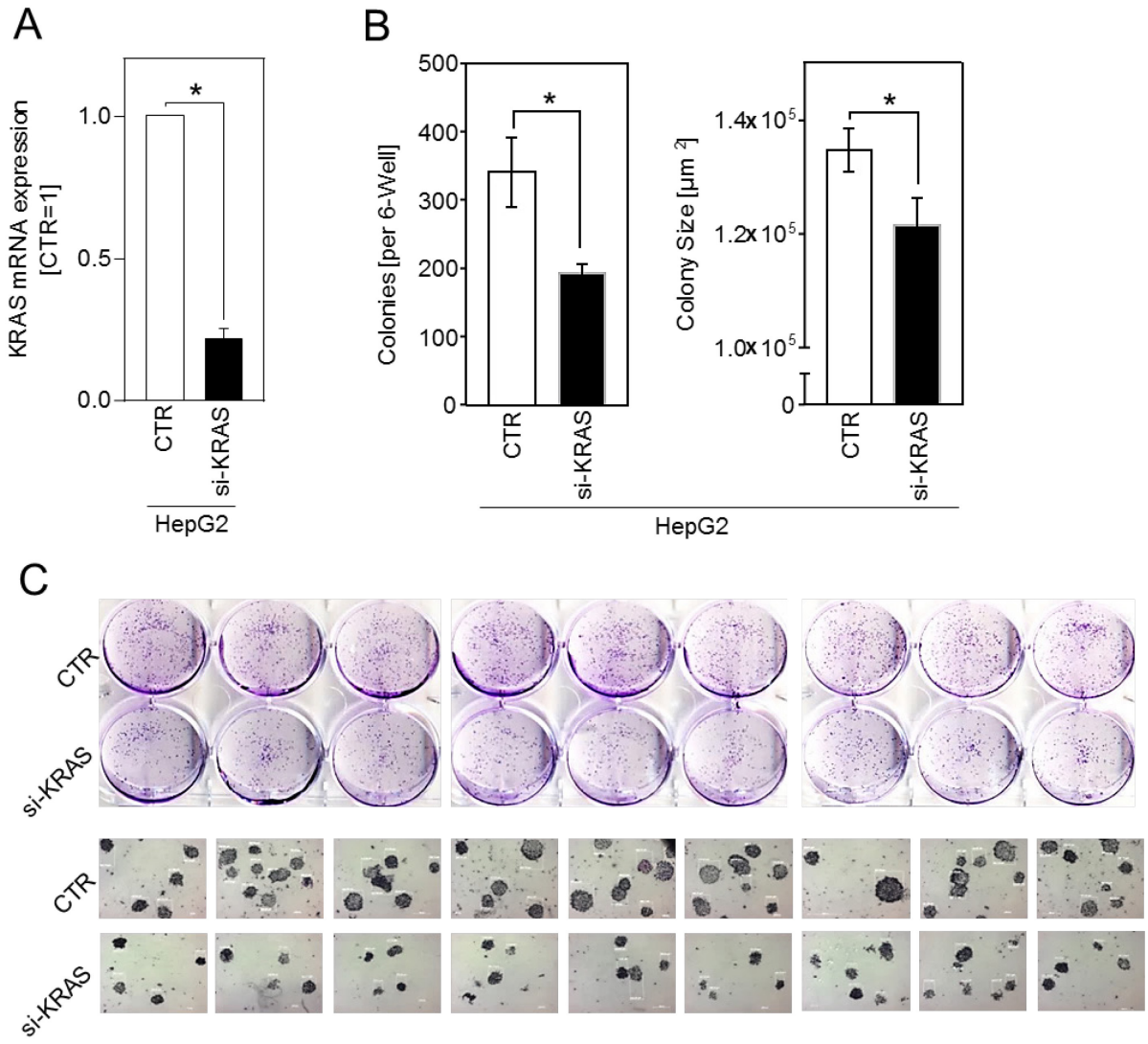

Figure S16 Confirmation of KRAS knockdown effects on anchorage-dependent and –independent clonogenicity in a third HCC cell line (HepG2). HepG2 cells were transfected with a control-si-RNA-Pool (CTR) or a si-RNA-Pool against KRAS (si-KRAS). **(A)** KRAS mRNA expression (qRT-PCR). **(B)** Quantification of colony number and colony size (anchorage-dependent clonogenic assay). (**C**) Exemplary images for both anchorage-dependent (upper images) and anchorage-independent (bottom images) clonogenicity assays. (*p<0.05 compared with control).

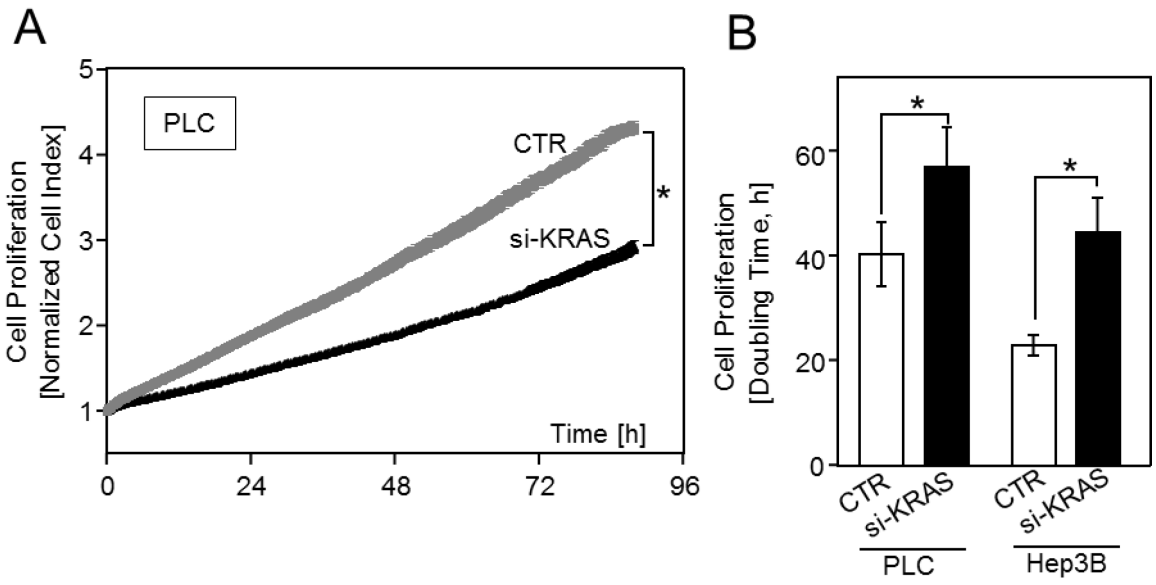

Figure S17 KRAS knockdown effects on proliferation in HCC.
Real-time cell proliferation analysis was performed after transfection with a control-si-RNA-Pool (CTR) or a si-RNA-Pool against KRAS (si-KRAS). Exemplary proliferation curves **(A)** and quantified "Doubling times" (summarizing the proliferative ability) **(B).** (*$p<0.05$ compared with control).

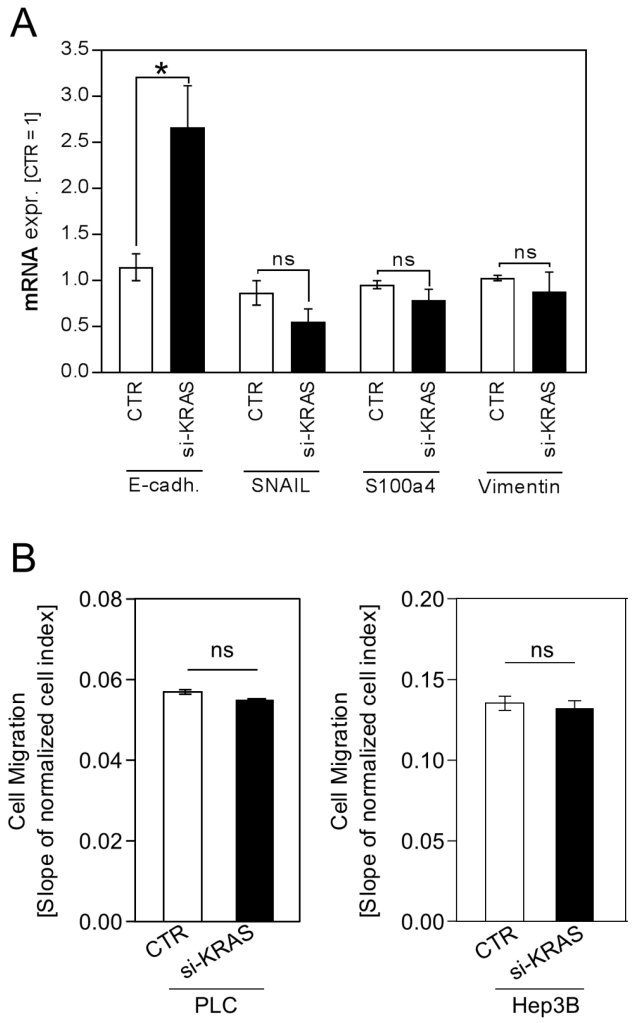

Figure S18 KRAS knockdown effects on epithelial-mesenchymal transition associated gene expression and cell migration.

(**A**) mRNA expression levels (E-cadherin, SNAIL, S100A4, VIMENTIN) in HCC cell lines (Hep3B and PLC) after si-RNA-pool-mediated KRAS knockdown (48 hours) as compared to control-transfected cells. (**B**) Cell migration after transfection with a control-si-RNA-Pool (CTR) or a si-RNA-Pool against KRAS (si-KRAS) as quantified by the xCELLigence real-time cell migration system in PLC (left panel) and Hep3B (right panel) HCC cell lines. (Ns: non-significant. *p<0.05).

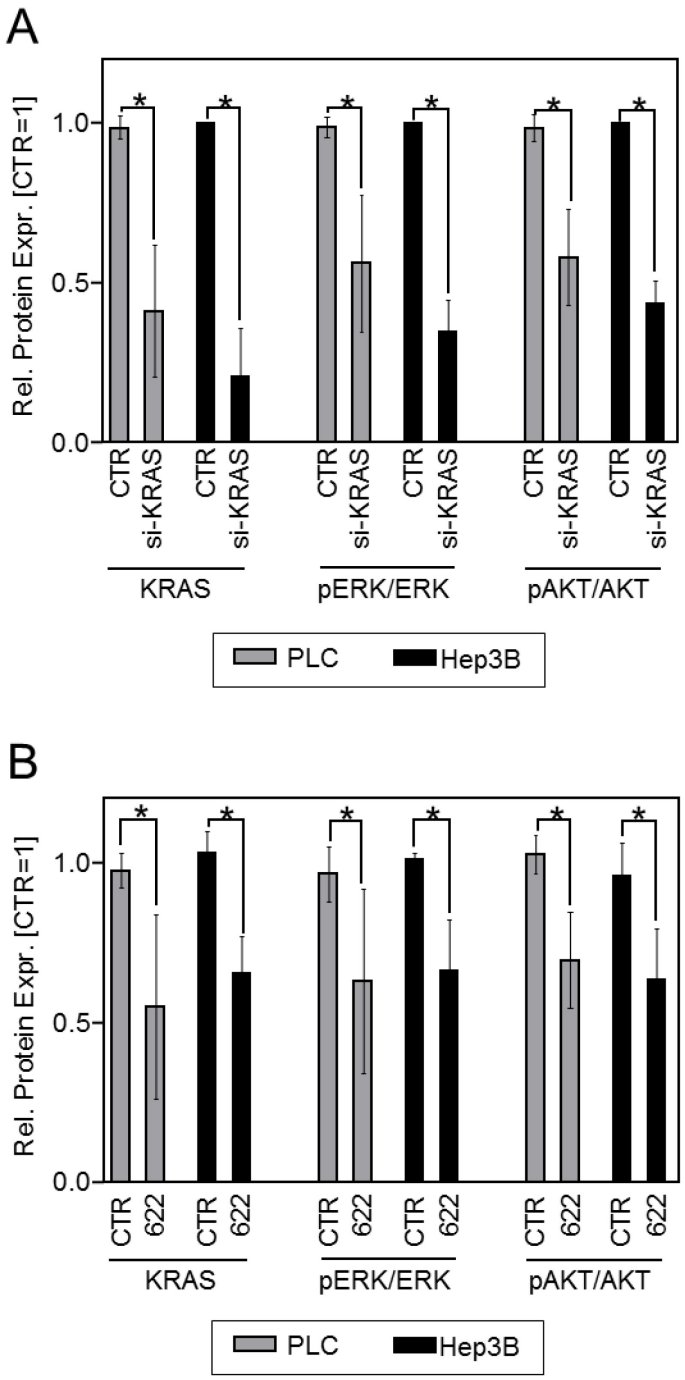

Figure S19 Western blot analysis after KRAS knockdown and miR-622-transfection in HCC.

Densitometric Western blot analysis of KRAS, pERK/ERK and pAKT/AKT protein expression are depicted. **(A)** PLC and Hep3B cells were transfected with a control-si-RNA-Pool (CTR) or a si-RNA-Pool against KRAS (si-KRAS). **(B)** PLC and Hep3B cells were transfected with a control-micro-RNA (CTR) or a miR-622-mimic (622). (*p<0.05 compared with control).

Figure S20/I

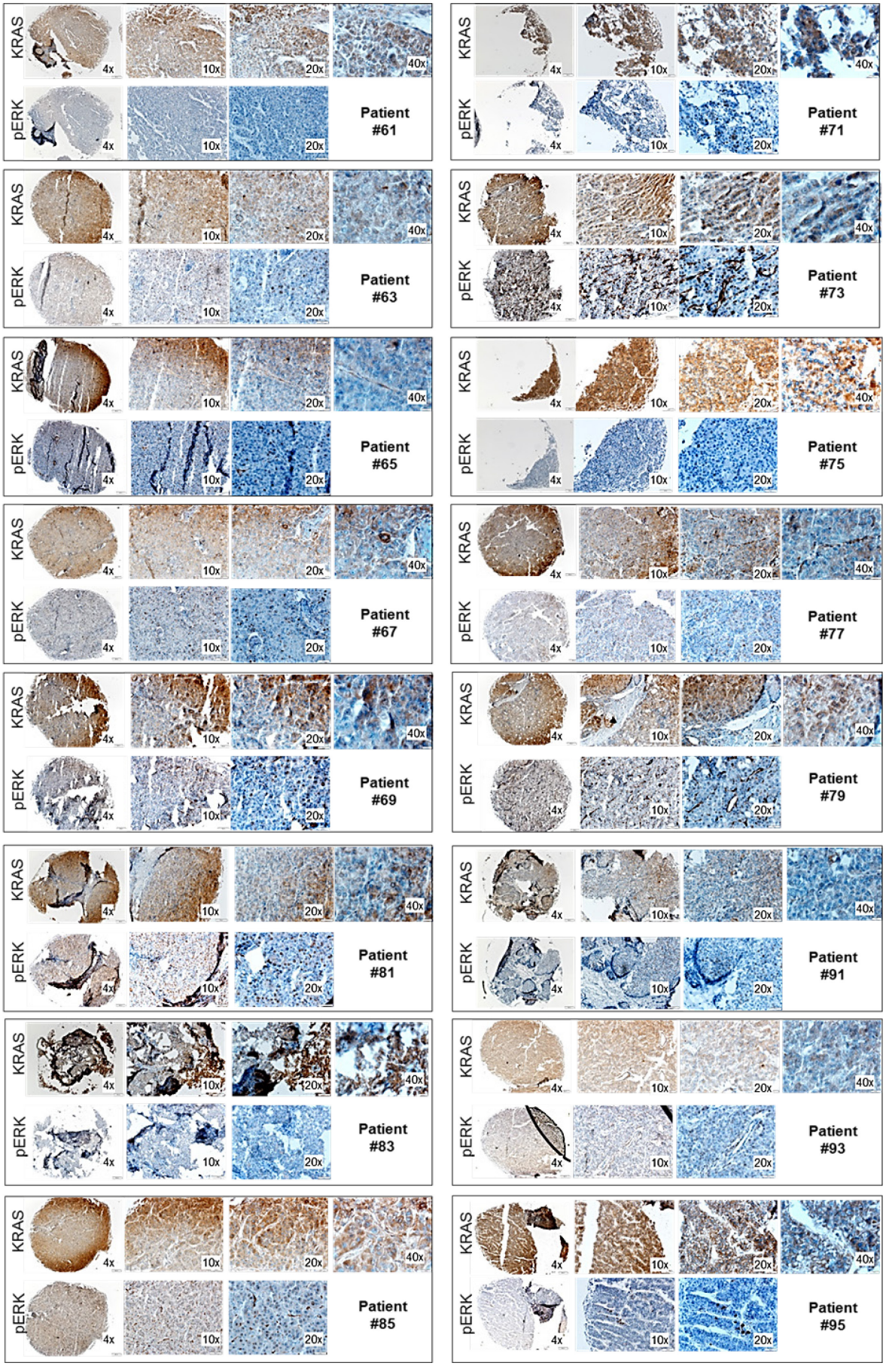
KRAS
pERK
4x
10x
20x
40x
Patient #61
Patient #71
Patient #63
Patient #73
Patient #65
Patient #75
Patient #67
Patient #77
Patient #69
Patient #79
Patient #81
Patient #91
Patient #83
Patient #93
Patient #85
Patient #95

Figure S20/II

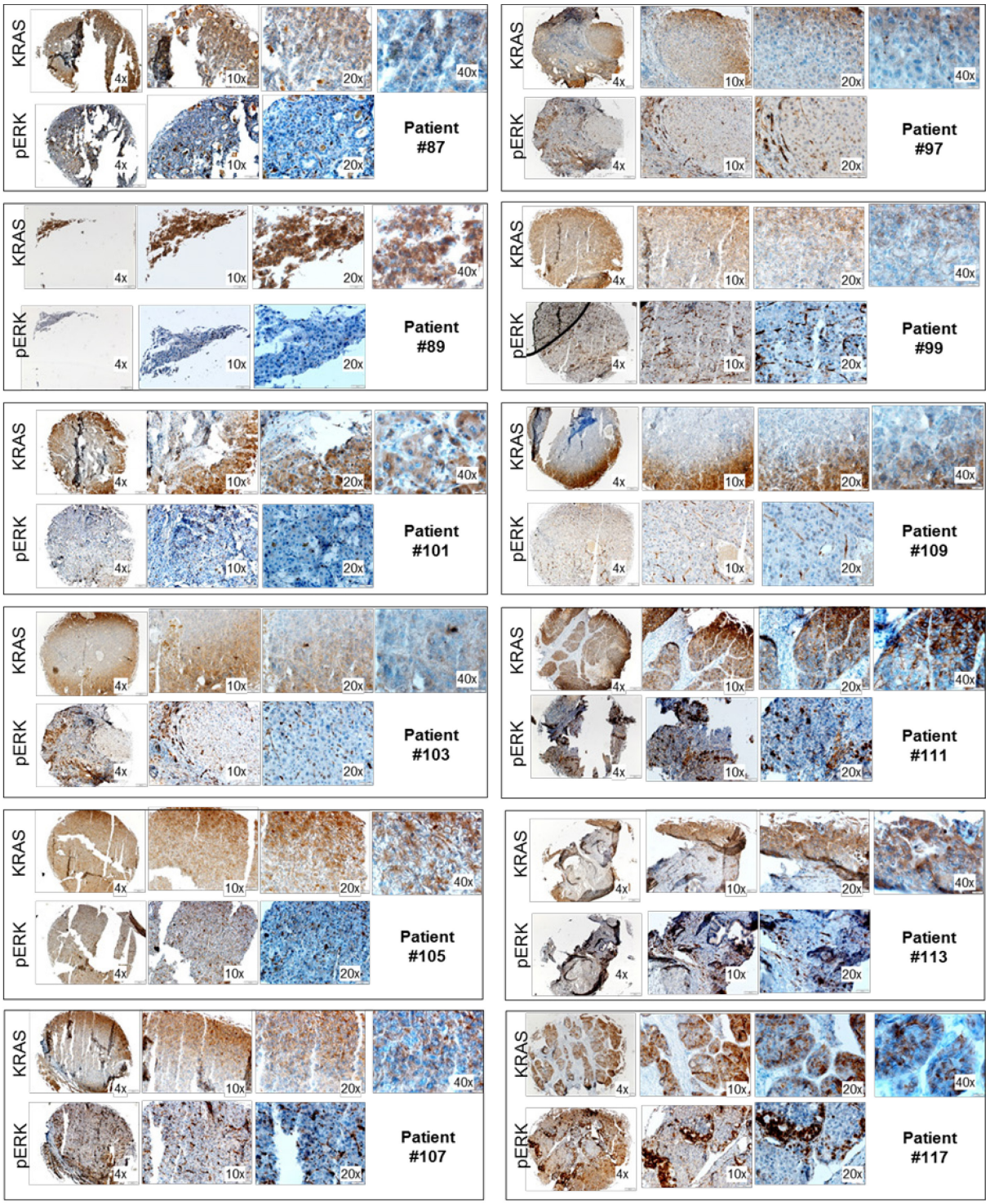

Figure S20/I+II Exemplary Tissue Micro Array Staining for KRAS and pERK in HCC.

Examples are shown for paired KRAS and pERK staining in HCC tissues using tissue micro array analysis.

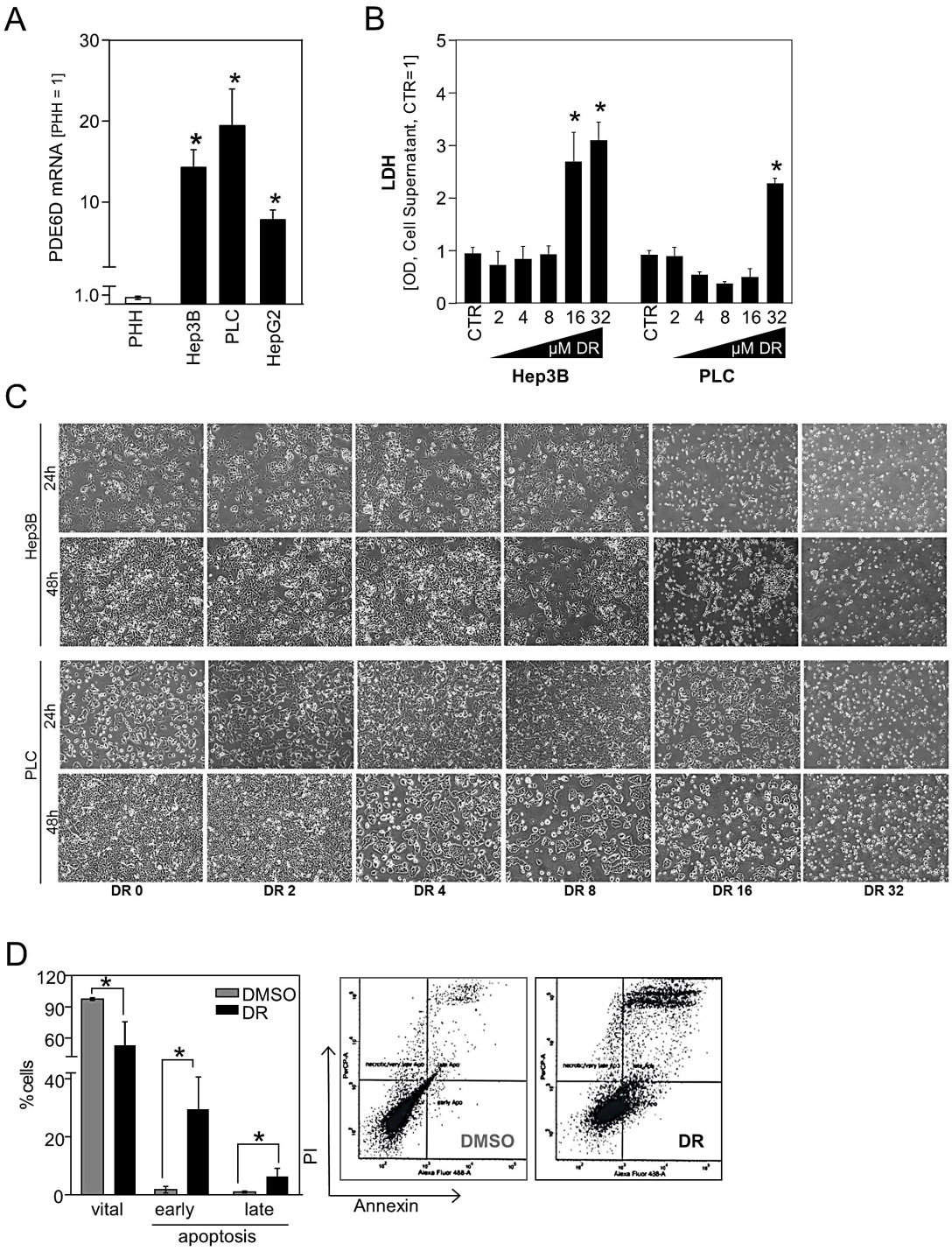

Figure S21 Cell toxicity and apoptosis induced by small molecule KRAS inhibition by deltarasin (DR) in HCC.

(**A**) PDE6D mRNA expression (qRT-PCR analysis) in primary human hepatocytes (PHH) as compared to HCC cell lines (Hep3B, PLC, HepG2). (**B-D**) HCC cells were treated with different doses of the small molecule KRAS inhibitor deltarasin. (B) Lactate dehydrogenase (LDH) release as quantified in cell supernatants of DR-treated (48 hours) HCC cells (Hep3B, PLC). (C) According exemplary images are depicted for PLC and Hep3B HCC cells for both 24- and 48-hour-treatment. (D) Fluorescence-activated cell sorting (FACS) analysis of apoptotic cells as performed using Annexin V and Propidium iodide (PI) staining and exemplary images (HepG2 HCC cells were treated with 8µM DR or DMSO for 16 hours). (*p<0.05 compared with control).

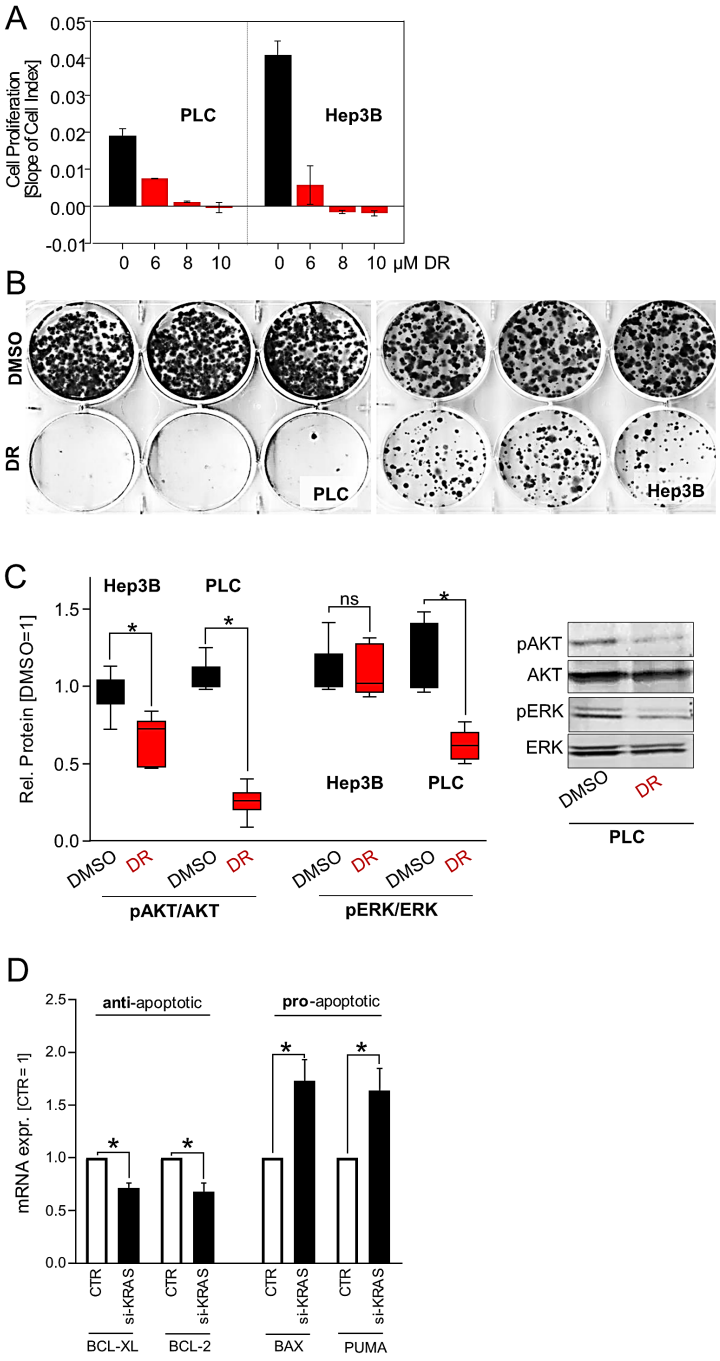

Figure S22 Function of KRAS inhibition on proliferation, clonogenicity, signaling and expression of apoptosis-related genes in HCC.

HCC cells were treated with different doses of the small molecule KRAS inhibitor deltarasin (DR) or DMSO. **(A)** Quantified real-time cell proliferation (slopes) (PLC and Hep3B). **(B)** Exemplary images of 3 replicate wells of an anchorage-dependent clonogenic assay (10 days, 5µM DR) (Hep3B and PLC). **(C)** Densitometric Western blot analysis for pAKT/AKT and pERK/ERK protein levels (PLC, Hep3B) and representative Western blot images (PLC). After starvation for 24 hours (cells were kept in serum free medium), cells were pre-incubated with 5 µM DR for 5 minutes, with subsequent stimulation (10 minutes) using fetal calf serum (FCS) and basic Fibroblast Growth Factor (bFGF, 5.0 ng/ml). (**D**) BCL-XL, BCL-2, BAX and PUMA mRNA expression as measured by qRT-PCR after KRAS knockdown in HCC (PLC, Hep3B) cells as compared to control (CTR) transfected cells. (Ns: non-significant. *p<0.05 compared with control).

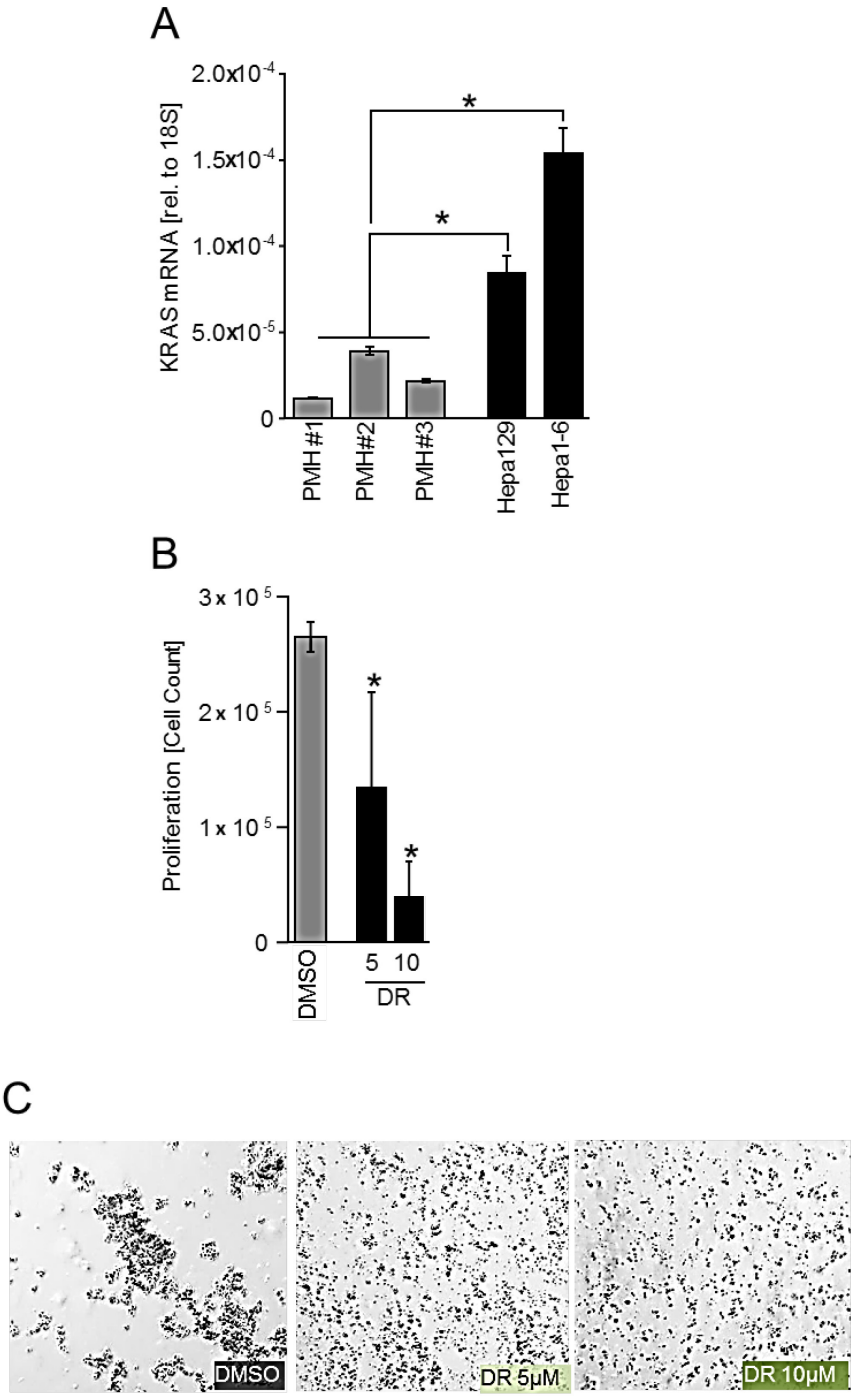

Figure S23 KRAS expression and effects of deltarasin-induced KRAS inhibition in murine Hepa129 HCC cells.

(A) KRAS mRNA levels as measured by qRT-PCR in murine HCC cell lines (Hepa129, Hepa1-6) as compared to primary murine hepatocytes (PMH) derived from three different mice. **(B,C)** Cells were treated with DMSO or deltarasin (DR) for 24 hours. Number of viable cells (Hepa129) as counted by microscopy after trypan blue staining (B) and exemplary images of treated cells (C). (*$p<0.05$ compared with control).

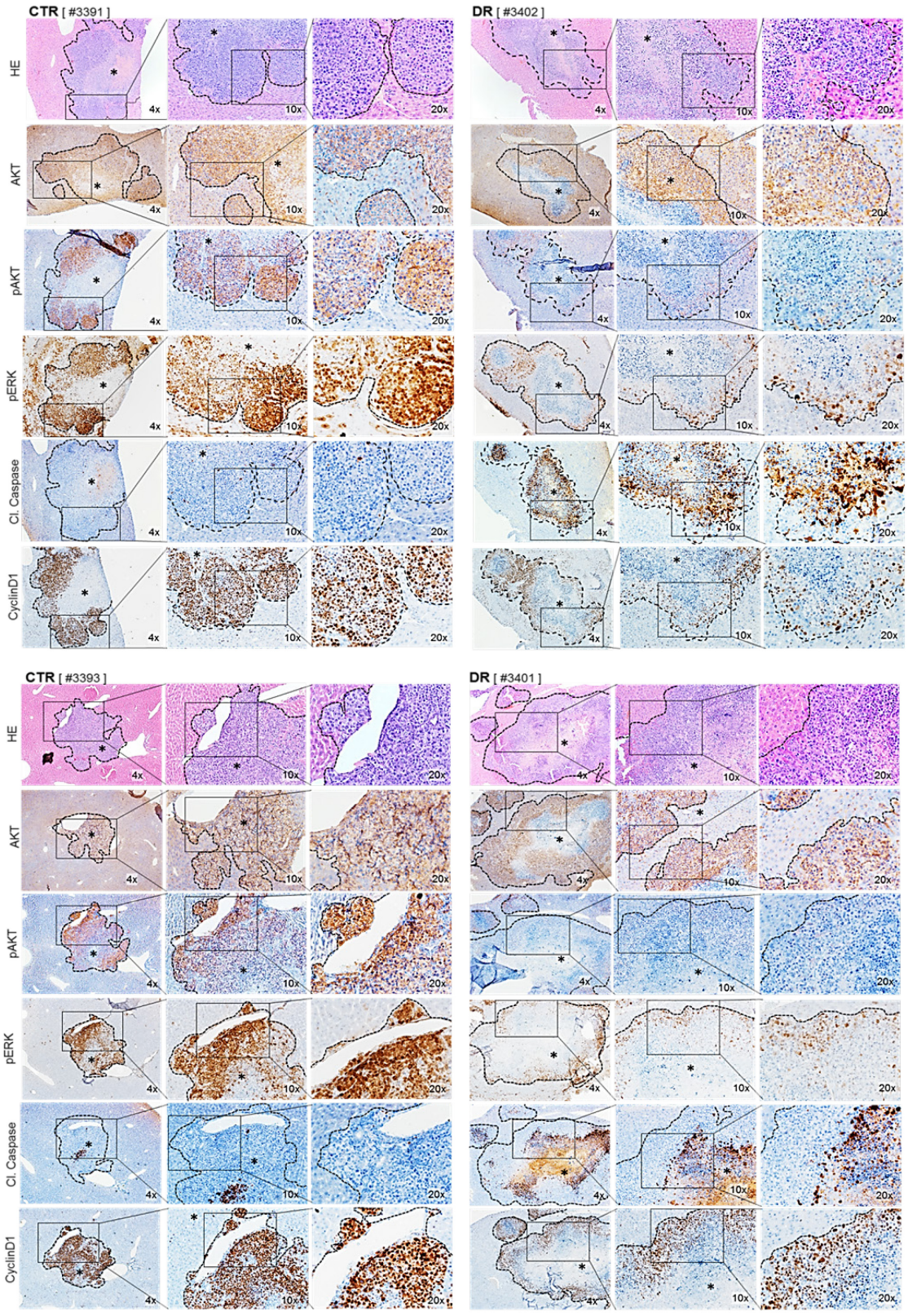

Figure S24 Deltarasin effects on HCC *in vivo*.
Exemplary images of immunohistological staining for HE, pAKT, pERK, cleaved Caspase 3, and CyclinD1. Hematoxylin-eosin (HE), AKT, pAKT, pERK, cleaved Caspase 3 and CyclinD1 staining of two exemplary tumors (derived from two different mice) from the control (CTR) and two exemplary tumors from the deltarasin (DR) group. Augmentations: 4-fold, 10-fold, and 20-fold. Dashed lines and stars ("*") mark the allograft tumors.

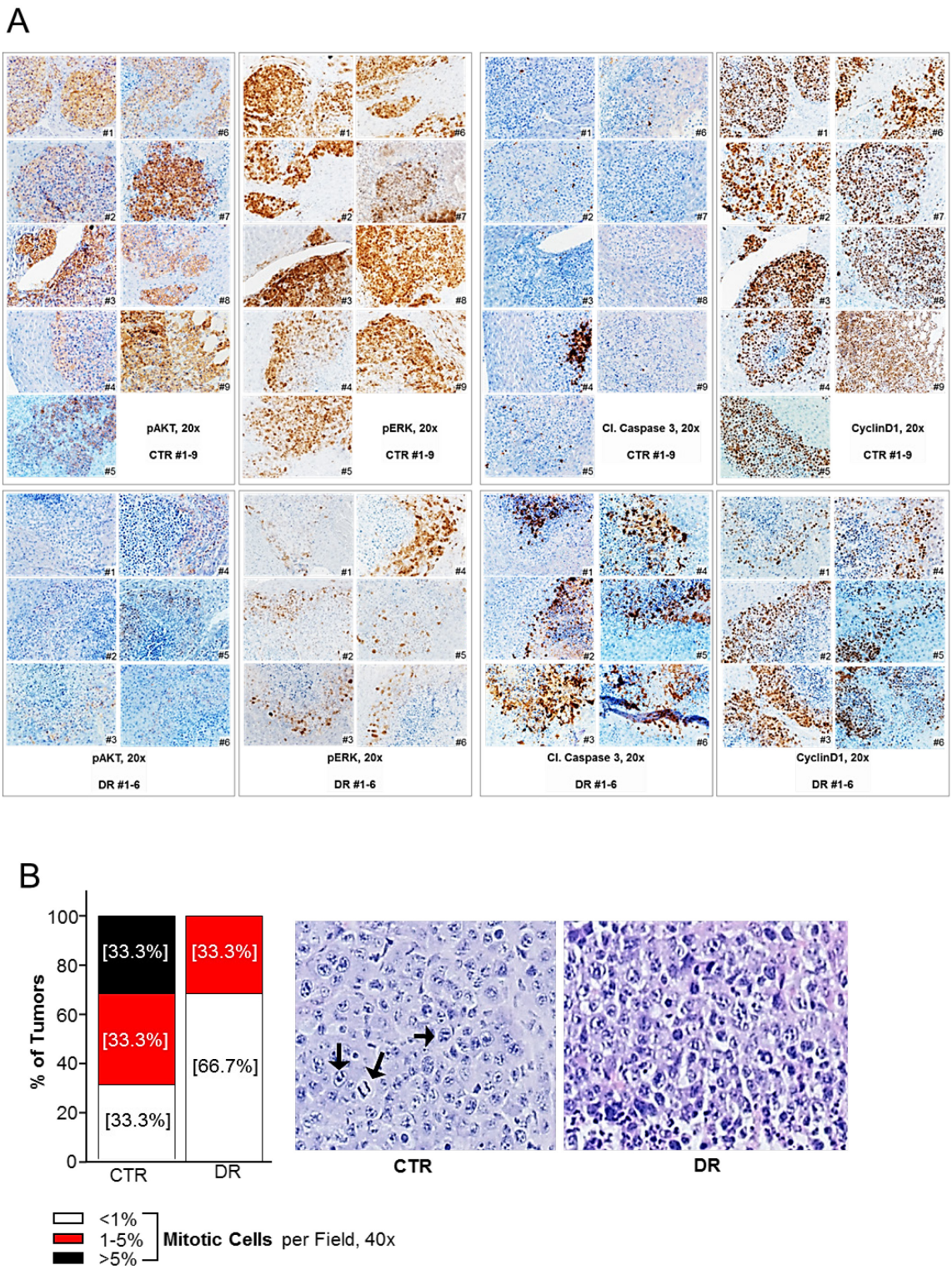

Figure S25 Deltarasin effects on HCC signaling and proliferation *in vivo*.
(A) Exemplary images (20-fold) for all allograft tumors of control and deltarasin (DR) treated mice. From right to left: pAKT, pERK, cleaved Caspase 3, and CyclinD1 staining. Depicted are exemplary 20-fold images for each tumor of the control (CTR, n=9) and the deltarasin group (DR, n=6). **(B)** Percentage depiction of mitotic HCC cells (classification <1%, 1-5%, and >5% mitotic cells per visual field with 40-fold augmentation) and exemplary images (20-fold), as analyzed in HE-stained tumors. Black arrows depict exemplary mitotic tumor cells.

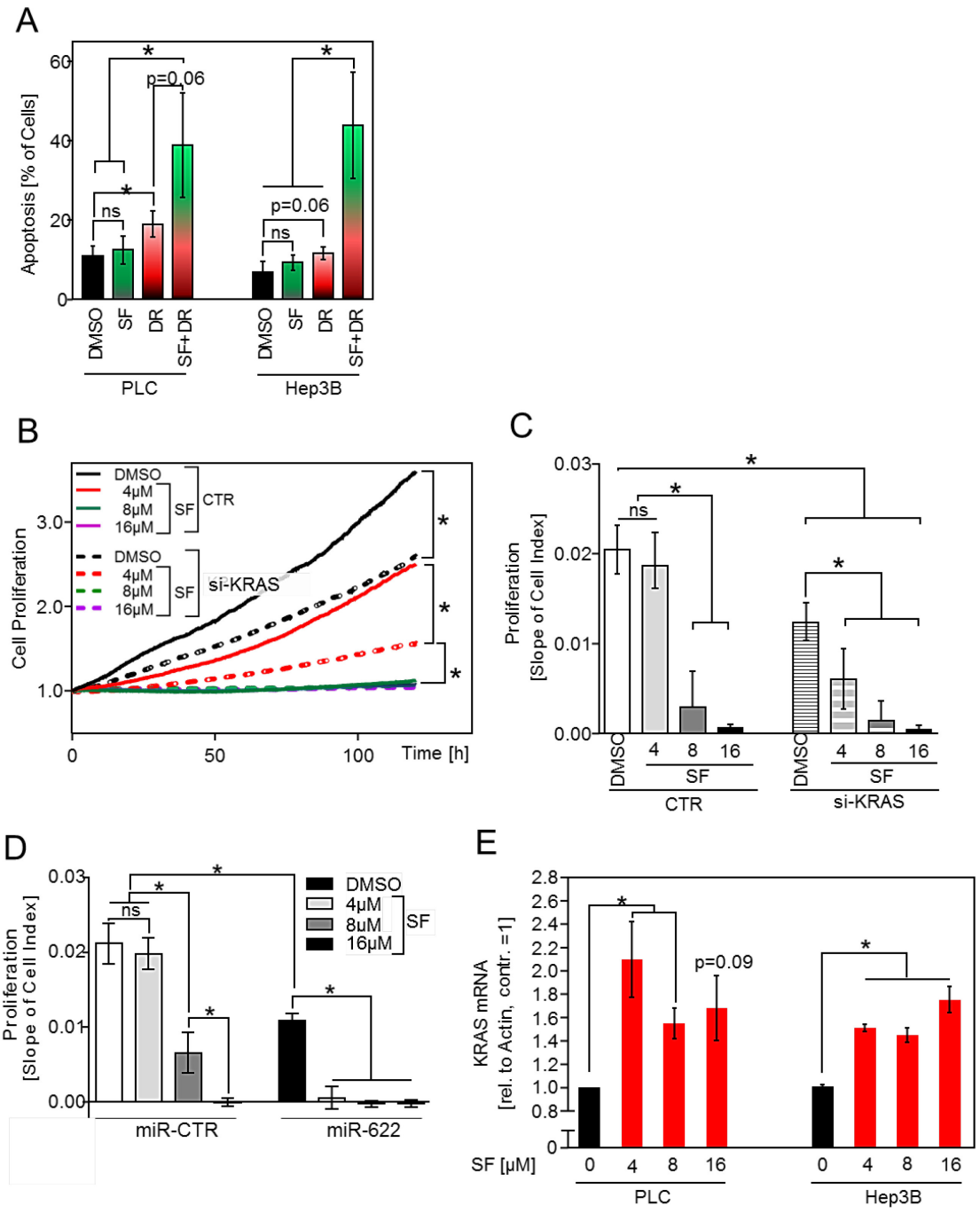

Figure S26 Effects of combination of sorafenib and KRAS inhibition in HCC. (A) Fluorescence-activated cell sorting (FACS) analysis of apoptotic cells (PLC, Hep3B) after treatment with DMSO, sorafenib (SF, 10μM), deltarasin (DR, 5μM), or a combination of SF+DR. Treatment was performed for 16 hours on confluent cells with subsequent FACS analysis. **(B,C)** Real-time cell proliferation (exemplary proliferation curve depicted in (B)), and according slopes of proliferation curves (C) of sorafenib (SF) treated Hep3B cells (0μM=DMSO, 4μM, 8μM, 16μM), with (si-KRAS) or without (CTR) KRAS repression. **(D)** Cell proliferation (slopes) of sorafenib (SF) treated PLC cells (0μM=DMSO, 4μM, 8μM, 16μM), with (miR-622) or without (miR-CTR) miR-622 transfection. **(E)** KRAS mRNA expression as measured by qRT-PCR after treatment of HCC cells (PLC, Hep3B) with no/low (0μM, 4μM) and high (8μM, 16μM) concentrations of sorafenib (SF) for 48 hours. (Ns: non-significant. *p<0.05 compared with control).

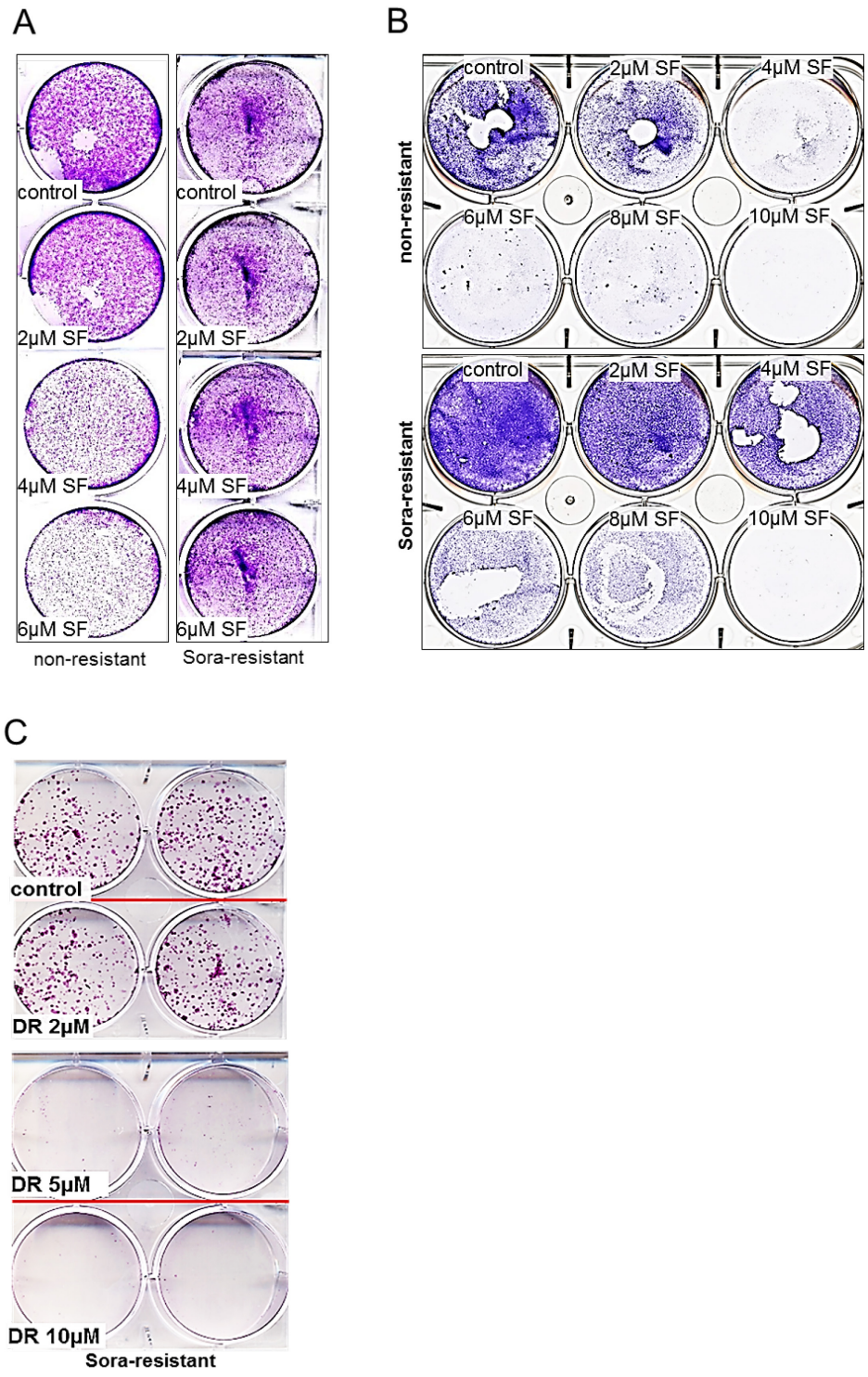

Figure S27 Effects of sorafenib and deltarasin on sorafenib (Sora)-resistant HCC cell proliferation and clonogenicity.

(A,B) Exemplary images for non-resistant (left side) and Sora-resistant (right side) Hep3B sub-confluent cells treated with 0, 2, 4, 6, 8 or 10μM sorafenib for 72 hours. **(C)** Clonogenic assays (exemplary images of two replicate wells for each condition) depicting sorafenib resistant Hep3B HCC cells. 24 hours after seeding, cells were treated with DMSO (control), or different doses of deltarasin (DR) (2, 5, and 10μM), and subsequently allowed to form colonies for 8 days before staining.

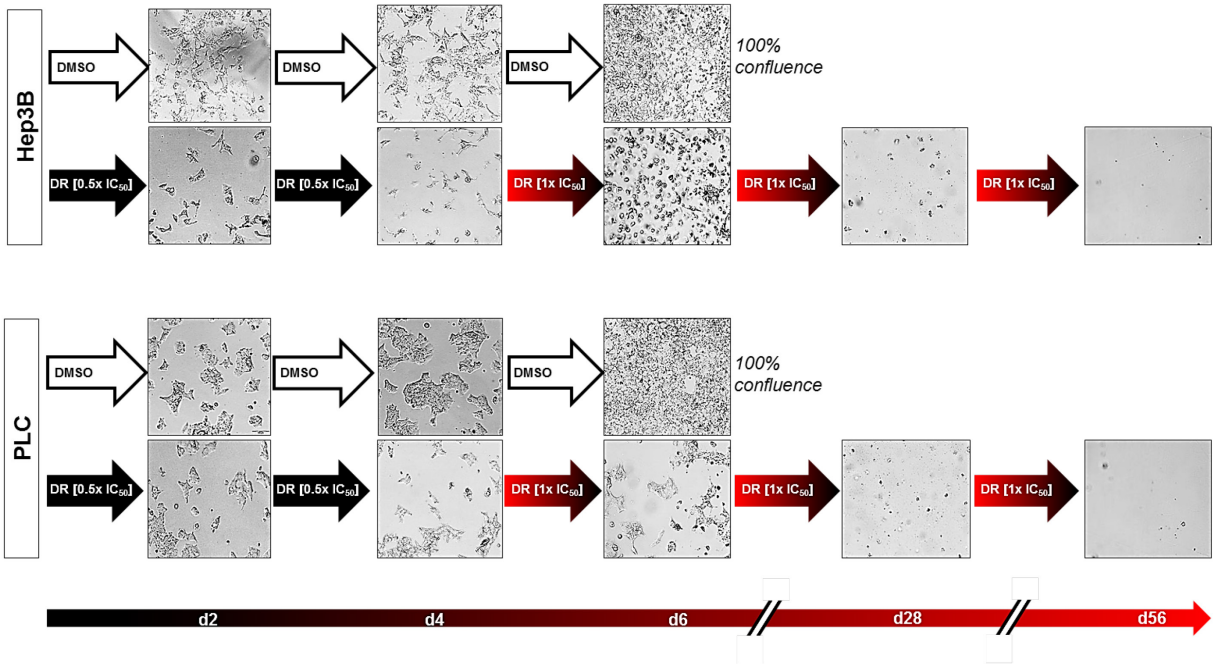

Figure S28 Effects of long term incubation with deltarasin on the potential emergence of drug resistant HCC cells.

The possible emergence of surviving tumor cells and drug resistance in response to deltarasin was evaluated. To generate resistance as described for other drugs, long term treatment of Hep3B and PLC cells using increasing deltarasin doses was performed, starting with low dose (0.5 x IC_{50}) (with 0.5µM-elevation-steps every 4 days). Moderate doses (1x IC_{50}) of deltarasin were sufficient to completely avoid the emergence of surviving tumor cells. ("d2 - 56": day 2 - 56).

Table S1. Clinico-pathological characteristics according to KRAS immunoreactivity of a tissue micro array (n=88).

Clinico-pathological characteristic	Categorisation	n (%)	KRAS IR		p*
			low (score 0-1)	high (score 2-3)	
Age at diagnosis					
	<60 years	32 (36.4)	10	22	0.498
	≥60 years	54 (61.3)	21	33	
	nd	2 (2.3)	0	2	
Gender					
	Female	12 (13.6)	3	9	0.524
	Male	74 (84.1)	28	46	
	nd	2 (2.3)	0	2	
Cirrhosis					
	yes	56 (63.4)	20	36	0.581
	no	18 (20.6)	8	10	
	nd	14 (16.0)	3	11	
Aetiology					
	HBC	7 (8.0)	2	5	0.759
	HCV	5 (5.6)	2	3	
	Alcohol	35 (39.8)	11	24	
	Others	1 (1.1)	1	0	
	nd	40 (45.5)	15	25	
Tumor stage					
	pT1	23 (26.1)	17	6	**<0.001**
	pT2	25 (28.4)	9	16	
	pT3	33 (37.5)	4	29	
	pT4	2 (2.3)	0	2	
	nd	5 (5.7)	1	4	
Histological grade					
	G1	31 (35.2)	7	24	0.131
	G2	45 (51.1)	20	25	
	G3	10 (11.4)	4	6	
	nd	2 (2.3)	0	2	
Tumor size					
	<5 cm	42 (47.7)	25	17	**<0.001**
	≥5 cm	30 (34.1)	2	28	
	nd	16 (18.2)	4	12	
Proliferation rate					
(Ki67 pos. cells)	<20%	43 (48.9)	25	18	**<0.001**
	≥20%	37 (42.0)	6	31	
	nd	8 (9.1)	3	5	
ERK-activation score					
(pERK pos. cells)**	<5%	31 (35.2)	30	1	**<0.001**
	5-20%	42 (47.7)	22	20	
	≥20%	13 (14.8)	1	12	
	nd	2 (2.3)	1	1	

*Fisher's exact test (two-sided); bold face representing p values <0.001.
**ERK activation score was determined in HCC tissues with low (score 0-1) or high (score 2-3) KRAS membrane localisation.
Nd, no data avaliable. IR, immunoreactivity.